Analysis of the Fisheries for Two Pelagic Carangids in Hawaii

Kevin C. M. Weng
Department of Oceanography
School of Ocean and Earth Science and Technology
University of Hawaii
Honolulu, HI

John R. Sibert
Joint Institute of Marine and Atmospheric Research
School of Ocean and Earth Science and Technology
University of Hawaii
Honolulu, HI

SOEST 00–04
JIMAR Contribution 00-332

ACKNOWLEDGMENTS

The authors wish to thank the Hawaii Division of Aquatic Resources for the fisheries data and digital maps used in the study, and the following individuals for assistance: Walter Ikehara, Reginald Kokobun, Kimberley Lowe, Jeffrey Polovina, Chris Boggs, Frank Kabakungen, Sam Pooley, Mark Merrifield, Craig Smith, Aunchalee Loscalzo, Matthew Parry, Jim Gharib, Joel Pfeiffer, and Catherine Adams. Additional funding was provided by the Fernando Leonida Memorial Scholarship.

This study was funded by cooperative agreement #NA67RJ0154 between the Joint Institute of Marine and Atmospheric Research (JIMAR) and the National Oceanic and Atmospheric Administration (NOAA). The views expressed herein are those of the authors and do not necessarily reflect the view of NOAA or any of its subagencies.

CONTENTS

TABLES

FIGURES

ABBREVIATIONS

B	biomass
$\hat{C}$	predicted catch
C	observed catch
CI	confidence interval (statistics)
CPUE	catch per unit effort
DAR	Division of Aquatic Resources
DF	degrees of freedom (statistics)
DLNR	Department of Land and Natural Resources
E	fishing effort
H0	null hypothesis
Ha	alternative hypothesis
k	population carrying capacity of the environment
K	somatic growth rate in von Bertalanffy growth equation
L	likelihood function
L_∞	average asymptotic length for a population in von Bertalanffy growth equation
Ln	natural logarithm
lb	pound
m	skew of surplus production
MLE	maximum likelihood estimation
MSY	maximum sustainable yield
NM	nautical mile
SD	standard deviation
P	probability of occurrence by chance (statistics)
ppt	part per thousand
q	catchability
r	population growth rate
t_0	age of fish at length zero in von Bertalanffy growth equation
t	time
T	t-statistic used in Student's *t* test (statistics)
U	catch per unit effort
W_∞	asymptotic weight in von Bertalanffy growth equation
θ	model parameters for maximum likelihood estimation
η	random variable used in model for maximum likelihood estimation
μ	mean

ABSTRACT

Fisheries for akule and opelu are important throughout their circumtropical range and are among the most productive nearshore fisheries in Hawaii. Commercial, community, and government interests have raised concerns of overfishing. In this study, a 30-year fisheries database is used for time series and spatial analysis. A model is developed which successfully diagnoses overfishing in an idealized scenario. This model indicates that both akule and opelu are exploited below maximum sustainable yield and are not threatened by the fisheries. Correlations with environmental time series show that the akule may be influenced by precipitation. Spatial analysis shows that the majority of the catch is taken from a small number of areas that receive the most effort. This analysis also indicates that the akule has sufficient site fidelity to allow localized reduction in CPUE due to fishing, while the opelu likely does not.

1 INTRODUCTION

This study presents an analysis of the commercial fishery for two small pelagic fishes in the main Hawaiian Islands. For each species, a literature review is conducted and a fishery catch and effort database is analyzed. The biology and fisheries of each species is described and analyzed. Spatial patterns in each fishery are identified, a search for correlations with climatic parameters is conducted, and the population dynamics are modeled. The health of each stock is assessed, based on biological parameters estimated from modeling.

Selar crumenopthalmus (akule) and *Decapterus macarellus* (opelu) have circumtropical distribution and fisheries for these species are important throughout this range (Dalzell and Penaflor 1989). In Hawaii, the fisheries for opelu and akule are among the most productive nearshore fisheries in the state. Between 1966 and 1997 (the period of available records) the annual catch of akule in the State of Hawaii averaged 612,000 pounds (wet weight), and the opelu catch 302,000 pounds, as calculated from Department of Land and Natural Resources data. Since 1991, the value of the Hawaiian catch of akule has exceeded $US 1 million (Iwai et al. 1996). For comparison, about 750,000 pounds of bottomfishes were landed from the archipelago in 1997 (DLNR 1999).

Concerns of overfishing have been raised by the commercial and recreational fishing interests, native rights representatives, the Hawaii Department of Land and Natural Resources (DLNR) Division of Aquatic Resources (DAR) and the Western Pacific Regional Fishery Management Council (WPRFMC).

For each species, the objectives of this study are to

- review biology and ecology (Chapter 2);
- develop time series of relevant fishery variables from the databases (Chapter 3);
- document the history of the fishery based on the fishery time series and available literature (Chapter 4);
- analyze spatial patterns and their biological and fishery significance (Chapter 5); and
- estimate biological parameters from the database and use these to assess the health of the stock (Chapter 6).

The term "variable" is used to refer to quantities that are empirically measured, and of which the "data" is comprised. In this study, the fishery data is comprised of the variables catch, effort, and catch per unit effort. The term "parameter" refers to quantities that cannot be empirically measured, and are estimated from the data. Both fishery and biological parameters are used. "Biological parameter" is used to refer to characteristics of the fishes and the ecosystem. There are stock-level biological parameters such as biomass, population growth rate, and carrying capacity as well as individual-level parameters such as maximum size, somatic growth rate, and fecundity. "Fishery parameter" is used to refer to characteristics of the fishery, such as the vulnerability of the target species to the particular methods used (the catchability).

2 BIOLOGY AND ECOLOGY OF AKULE AND OPELU

2.1 Introduction

Akule and opelu are members of the Carangid family, which have achieved broad success in nearshore tropical and subtropical marine environments worldwide. These species have circumtropical distribution and fisheries for them are important throughout this range (Dalzell and Penaflor 1989).

2.2 Morphology and Ontogeny

Detailed information of the early ontogeny of the akule is reported in two studies in which fish are reared in captivity from spawned eggs (Iwai et al. 1996, Podosinnikov 1990). No such research has been conducted for the opelu. Spawned eggs of the akule average 630 μm in diameter and are transparent and buoyant in salinities of 32-35 ppt. Newly hatched prolarvae are 1.3 to 1.5 mm in length, with no pectoral fins and a yolk sac protruding anterior to the head. The prolarvae hang suspended from the surface of the water and drift passively. Swimming ability presumably develops with growth, but the time required is unknown. It is thought that the larval phase lasts about four months. This conclusion is based upon two pieces of information. First, the spawning season for akule generally begins in April, and the first juveniles usually enter coastal waters in July, an interval of 4 months. Second, the estimate of t_0 in the Von Bertalanffy growth equation is -4 months (Kawamoto 1973). This parameter represents the age of the fish at length zero if it had the growth trend shown from the age of the first individuals for which data exists (i.e., new recruits). The Von Bertalanffy growth equation is discussed further in section 2.1. It is possible that a third estimate of pelagic larval duration could be obtained from the inspection of otoliths, although the settlement marks present in benthic fishes may not be present in a pelagic fish such as akule or opelu.

As shown in Figure 1, both species have fusiform bodies, small mouths, and scutes characteristic of the carangid family. Figure 1 also shows detail of important morphological characteristics. A detailed morphological description of the akule is available from Schultz et al. (1953) for *Trachurops crumenopthalmus*. A description of the opelu is available from Gushiken (1983).

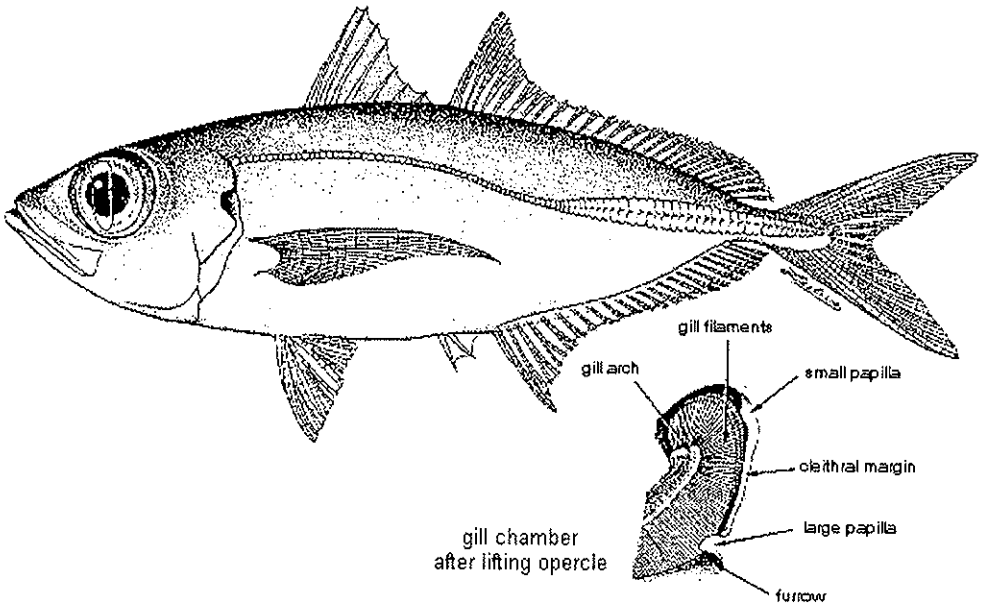

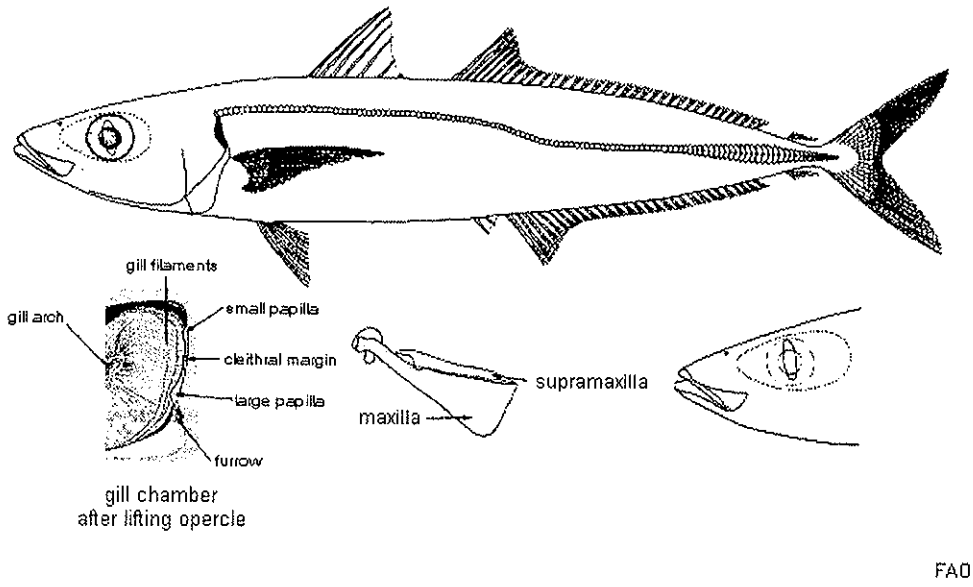

Figure 1. Adult Specimens of *Selar crumenopthalmus* (top) and *Decapterus macarellus* (Source: Food and Agricultural Organization)

2.2.1 Growth

Akule and opelu have high growth rates, although the estimates made in this study indicate that the growth of the akule is about three times faster than the growth of the opelu. Figure 2 shows von-Bertalanffy growth curves (von Bertalanffy 1957) for the two species. For the akule, the parameters *L infinity* (maximum asymptotic average length for the population in mm) and *K* (somatic growth constant, month^{-1}) were calculated by Kawamoto (1973) using growth-time increments from tagging experiments fitted to the von Bertalanffy equation. Tag-recapture experiments allow measurement of growth in the natural environment for the same individuals.

The only published work to estimate somatic growth rates for opelu (Yamaguchi 1953) used the Petersen method (Petersen 1895) in which modes in the population are followed through time and assumed to be cohorts. The growth occurring between sampling times for a mode is then assumed to be the growth occurring for a cohort. Since the growth measurements occur on different individuals at each time, the Petersen method contains an additional source of error and is less reliable than tag-recapture methods.

Yamaguchi's work preceded the development of the von Bertalanffy equation, so I have used his growth-time increments to fit a von Bertalanffy growth equation and estimate the parameters *L infinity* and *K*.

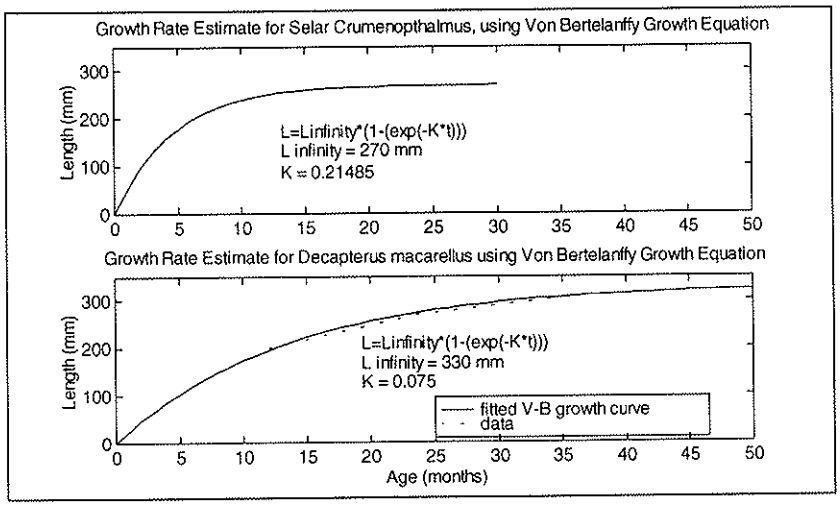

Figure 2. von Bertalanffy Curves for *S. crumenopthalmus* and *D. macarellus*. These curves show the *S. crumenopthalmus* grows faster than *D. macarellus*, and has a shorter asymptotic length.

The plots in Figure 2 agree closely with others available in the literature (Froese and Pauly 1998). The growth rate for akule (K = 0.21/month, or 2.58/year) is very high and indicative of a highly productive species. That obtained for the opelu is lower (K = 0.075/month). The akule approaches 95% of asymptotic length in one to two years, the opelu in two to three years.

2.2.2 *Life Cycle*

The two species have somewhat similar life cycles. They are heterosexual, iteroparous, and have spawning aggregations during which promiscuous breeding occurs with external fertilization. They spawn pelagic eggs that hatch to larvae with a four-month pelagic phase (as discussed under *Larval Stage*, above). At the end of the pelagic larval phase, the juveniles migrate inshore and recruit into the adult schools that live in nearshore waters (Kawamoto 1973). During these migrations, juvenile akule, or hahalalu, form schools that run along the shoreline. Although the adults live in shallow water, they are considered pelagic because they do not maintain close association with substrate. The range of movement of akule is limited based on tagging studies (Kawamoto 1973). The opelu is found further offshore than the akule.

The gonads of the akule are generally mature or spent during April through November, which is thought to be their spawning season. The akule becomes sexually dichromatic during spawning season on the soft portion of the anal fin, which is black in males and white in females (Clarke and Privitera 1995). Spawning in captive fish occurs during the night with the majority of the spawns occurring in the pre-dawn hours (Iwai *et al.* 1996). Mass spawning in the Gulf of Aden generally occurs at night (Podosinnikov 1990).

The akule is a multiple spawner as evidenced by the bimodal size frequency of oocytes observed during ovarian biopsies (Clarke and Privitera 1995, Iwai et al. 1996) as well as by the multiple recruitment size classes appearing during one year (Dalzell and Penaflor 1989, Kawamoto 1973). A bimodal size distribution of oocytes indicates that the fish is preparing the next batch even as the current batch is ripening.

The opelu spawning season lasts from March or April to August (Clarke and Privitera 1995, Yamaguchi 1953). It is believed to spawn in the same areas regularly occupied by adults. Large schools or 'bait-balls' may occur during spawning season, in which the fish rub each other's undersides with a flickering motion that is believed to be a spawning behavior. Catches from such aggregations are dominated by ripe or spent males; Yamaguchi (1953) attributes the absence of females to their non-response to bait or chum rather than their movement to spawning grounds without the males, but no evidence supports this. The spawning frequency of the opelu is uncertain. Yamaguchi (1953) states that the oocyte size distribution was unimodal; however, Clarke and Privitera (1995) provide inconclusive evidence that the distribution may be bimodal.

The relevant biology of the two species is summarized in Table 1.

Table 1. Biology of Akule and Opelu

	Akule	Opelu
Size at Maturity	200 mm SL	245 mm SL 170 mm[1]
Age at Maturity	7 month[4]	18 months[4]
Spawning Season	April-October	April-August
Spawning Frequency	1 per 3 days 5-10 times per year[2]	unknown
Batch Fecundity	92,000 96,000 to 121,000[2]	136,000 82,000 for 200 mm fish[1]
Growth (k)	0.21/month[3]	0.075/month[4]
Maximum size (L infinity)	270 mm[3]	330 mm[1]

Clarke and Privitera 1995, unless otherwise noted

(1) Yamaguchi 1953

(2) Iwai *et al.* 1996

(3) Kawamoto 1973

(4) Estimated with von Bertalanffy equation

2.3 Distribution and Habitat

2.3.1 Akule

The akule is circumtropical. In the Pacific, it is found from southern Africa to southeast Asia; northeast to southern Japan and Hawaiian Islands; south to New Caledonia and Rapa; and eastwards from Mexico to Peru, including Galapagos Islands (Chirichigno 1974). In the Western Atlantic, it is found from Nova Scotia, Canada and Bermuda to Rio de Janeiro, Brazil; and throughout the Gulf of Mexico and the Caribbean Sea (Cervigón 1993). In the Eastern Atlantic, it occurs from Cape Verde Island to southern Angola (Smith-Vaniz et al. 1990).

The akule is generally found in inshore waters and shallow reefs to 170 m (Smith-Vaniz 1986). The species prefers clean, clear, insular waters (Cervigón 1993) but is occasionally found in turbid waters (Smith-Vaniz 1995). The akule travels in compact groups of hundreds of thousands of fish (Cervigón 1993). Observations based on current speed and direction and lunar phase indicate that these fishes school and remain in areas where abundant zooplankton food resources are concentrated in lee eddies (Tobias 1987). Tagging experiments indicate that there is very little movement between populations in the northern, western, and southern waters of Oahu, Hawaii (Kawamoto 1973). The larvae of these species are pelagic (Kawamoto 1973). In a study of ichthyoplankton vertical distribution, larvae of these fishes were caught at all stations of east-west transects off Kahe Point and Kaoio Point (Oahu, Hawaii) at depths of 0-80 m. Stations were at 1, 5, and 15 km offshore and sampling occurred to a depth of 200 m (Boehlert and Mundy 1996).

2.3.2 Opelu

The opelu is also circumtropical. In the Western Atlantic, it is found from Nova Scotia, Canada and Bermuda to approximately Pernambuco, Brazil. It appears to be absent from the Gulf of Mexico (Cervigón 1993). In the Eastern Atlantic, it occurs in St. Helena, Ascension, Cape Verde Islands, and Gulf of Guinea (Smith-Vaniz et al. 1990); and in the Azores and Maderia Islands (Smith-Vaniz 1986). In the Indian Ocean, the opelu is found in South Africa, Seychelles,

Mascarenes, Red Sea, Gulf of Aden and Sri Lanka (Smith-Vaniz 1984). In the Eastern Pacific, it ranges from the Gulf of California and Revillagigedo Islands in Mexico to Ecuador (Smith-Vaniz 1995).

The opelu forms schools in mid-waters of deep lagoons, coastal bays, or offshore waters and generally stays away from coral reefs. It is sometimes encountered near the surface (Smith-Vaniz 1995). The larvae of opelu are pelagic and have been found 80 miles from the shore of Oahu, Hawaii (Yamaguchi 1953). In a study of ichthyoplankton vertical distribution, larvae of these fishes were caught at all stations of east-west transects off Kahe Point and Kaoio Point (Oahu, Hawaii) at depths of 0-80 m. Stations were at 1, 5, and 15 km offshore and sampling occurred to a depth of 200 m (Boehlert and Mundy 1996).

2.4 Trophic Relationships

The akule and the opelu occupy intermediate niches in the marine ecosystem because they are predators of macrozooplankton and important prey of larger pelagic fishes.

2.4.1 Akule

Primarily a nocturnal fish, the akule feeds on shrimp, other invertebrates, and forams when inshore and zooplankton and fish larvae when offshore (Cervigón 1993). In Hawaii, small fishes (anchovies, holocentrids and others), copepods, crab megalops, stomatopods, shrimps, and other planktonic crustaceans comprise the majority of the akule's adult diet (Kawamoto 1973). The akule is preyed upon by tunas, large carangids, and billfishes that are in nearshore waters (Kawamoto 1973).

2.4.2 Opelu

The adult opelu feeds mainly on macroplanktonic crustaceans such as hyperiid amphipods, crab megalops, various crustacean larvae, chaetognaths, and fish larvae (Yamaguchi 1953). The opelu is prey for yellowfin, skipjack, and bigeye tuna; wahoo (ono), dolphin fish (mahimahi), kawakawa, striped marlin, and rainbow runner (Yamaguchi 1953). The adult opelu is commonly found in the stomach of the yellowfin tuna in the vicinity of islands, but has not been so recorded for tuna captured in the remote pelagic environment. However, juvenile opelu commonly occur in large schools in the pelagic ocean, where schools of skipjack tuna feed on them (Yamaguchi 1953).

2.5 Summary

The akule and the opelu are members of the Carangidae family and support important commercial and subsistence fisheries throughout their circumtropical ranges. Both species are heterosexual, iteroparous, and have spawning aggregations during which promiscuous breeding occurs with external fertilization of free-floating pelagic eggs. Detailed study of the early ontogeny of the akule has shown rapid embryonic development and a four-month pelagic larval phase prior to recruitment to nearshore adult stocks. Both species spawn in spring, summer, and fall. The akule spawns multiple times per season; this frequency is unknown for the opelu. Both species are highly fecund and have high somatic growth rates, the akule's being faster than the opelu's. The akule and opelu occupy an intermediate position in the marine ecosystem, being

predators of macrozooplankton and prey of larger pelagic fishes. As such, these small pelagic species form a trophic link between the nearshore environment from which they feed, and the offshore pelagic environment occupied by many of their predators.

3 DERIVING FISHERY VARIABLES FROM THE DATABASES

3.1 Introduction

The databases used in this study allow the calculation of catch, effort and catch per unit effort (*CPUE*), which are the basic fishery variables from which biological and fishery parameters are estimated. This chapter describes the methods used to calculate these variables, along with the quality control methods used to filter out records that introduce bias and error. The initial calculation of variables results in the time series referred to as "raw," while the time series calculated with various quality control criteria are referred to as "refined.

3.2 The Databases

The primary data sources for this project are the daily time series of catch collected by the DAR over the past 30 years. The databases for opelu and akule contain the fields described in the table below.

Table 2. DAR Database Fields

Inputs DAR Database from 1966-1997 ~ 180,000 records	
Boat license	An individual license number for a boat. This allows calculation of the number of boats in the fishery.
Year	
Month	
Day	Allows the calculation of an index of effort based upon boat-days of fishing.
DAR Area	All nearshore waters in the Main Hawaiian Islands have been divided into areas, to which catch is assigned. This allows spatial analysis of catch, effort and *CPUE*.
Method	HANDLINE and NET. The NET category includes purse seine, surround net, gill net, and hoop net.
Species	AKULE or OPELU
Catch (lb.)	

3.3 Methods

3.3.1 Raw Fishery Variables

Time series of catch, effort, and *CPUE* can be calculated from the original DAR databases. The time series calculated with the methods described in this section are referred to as raw. The method of calculating refined time series is described in Section 3.3.2.

Summing the individual catch records into annual bins creates an annual time series of catch. Effort is not explicitly defined because DAR did not include a field in their reporting forms for fishing effort. Therefore, it is assumed that each report (i.e., each record in the database) represents a single fishing trip. Such an assumption is reasonable because the fishery operates in nearshore waters with predominantly single day trips. Errors are likely to occur due to non-reporting or reporting of multiple trips at once, rather than from the occurrence of multi-day trips. Given this assumption, the number of records can be summed to produce and index of effort, the "boat-day." Counting the number of records in each year of the time series gives the boat-days of effort exerted during the year. *CPUE* is calculated by dividing catch by the effort.

The catch and effort can also be summed or averaged over the management areas used by DAR to categorize spatial distribution of the fishery. DAR has defined management areas for nearshore Hawaiian waters (see Chapter 5).

The number of licenses issued each year can be summed to produce a time series of the number of boats in the fishery.

3.3.2 Refined Fishery Variables

The above time series may suffer from biases introduced by the data collection methods of DAR or the reporting habits of fishermen. A number of refinements are immediately apparent from the data, while others are discerned only after closer inspection. The various refinements are as follows.

- *Zero license number fields*—DAR does not use zero as a license number so these records are not traceable to a particular boat. Therefore, they are considered to be suspect and removed from the refined time series.
- *Zero day and month fields*—These records were recorded without a time and are considered suspect. Therefore, they are removed from the refined time series.
- *Abnormal daily CPUE*—The *CPUE* for each day of the month, averaged over all years and all areas, is higher at the end of the month than in all other days. This pattern is likely to be due to the reporting of multiple trips at the end of the month as fishermen catch up on backlogged reports.

These refinements remove only 3% of the total number of records for akule and 6% for opelu. They remove error and bias but do not greatly reduce the size of the database.

3.3.2.1 Zero License Numbers

In addition to the suspect days, some records in the original database have license numbers of zero. These records are not connected to any particular boat and are therefore considered to be suspect. Such records are filtered out in the time series produced.

3.3.2.2 Zero Day, Month and Year Records

For both akule and opelu, the database contains records with date fields having a value of zero. The records accumulate all reports for which the date was not specified. These reports are considered biased and are excluded in calculating the refined time series.

3.3.2.3 Abnormal Daily CPUE—Backlogged catches

Fishermen sometimes fall behind in reporting catches and then report multiple days catch at the end of the month to catch up (Chris Boggs, National Marine Fisheries Service, personal communication). If this is the case, we expect the *CPUE* for these days to be higher than other days. There is not an obvious biological reason that *CPUE* would increase at the end of the month. Therefore, the *CPUE* for each day of the month, averaged over all years, is analyzed. The daily *CPUE* for akule is slightly higher on day 31. The distribution of days 1 to 30 is normal, with day 31 being an outlier (defined as 1.5*IQR beyond a quartile).

The daily *CPUE* for the opelu showed a peak for the last two days of the month. A normal distribution exists for days 1-29, with days 30 and 31 being outliers as defined above. Based on these distributions, days with abnormal *CPUE* are considered to be biased data and are excluded from the refined version of opelu *CPUE*.

3.3.3 Time Series from High Catch Areas

The full database (including refinements above) contains records from all areas, whether they make important contributions to the fishery or not. To eliminate variability caused by reports from less productive areas, which may not be important in the fishery, time series are generated from the DAR areas showing the highest catch levels only.

3.4 Results

The data products produced for this study using the DAR database are listed below.

- Annual time series of catch, effort, and *CPUE* for each species integrated over all DAR areas.
- Spatial distribution of catch, effort, and *CPUE* within DAR areas for the entire period on record.
- Annual time series of number of boats in the fishery for all DAR areas.

3.4.1 Raw Time Series

The time series for akule and opelu using the raw data are shown in Figures 3-6.

3.4.1.1 Akule

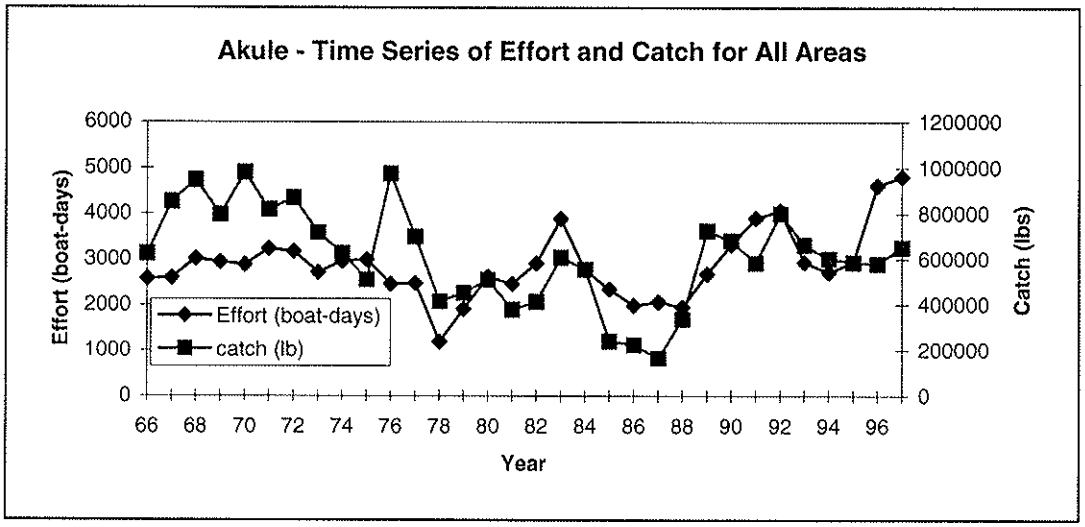

Figure 3. Time Series of Akule Effort and Catch

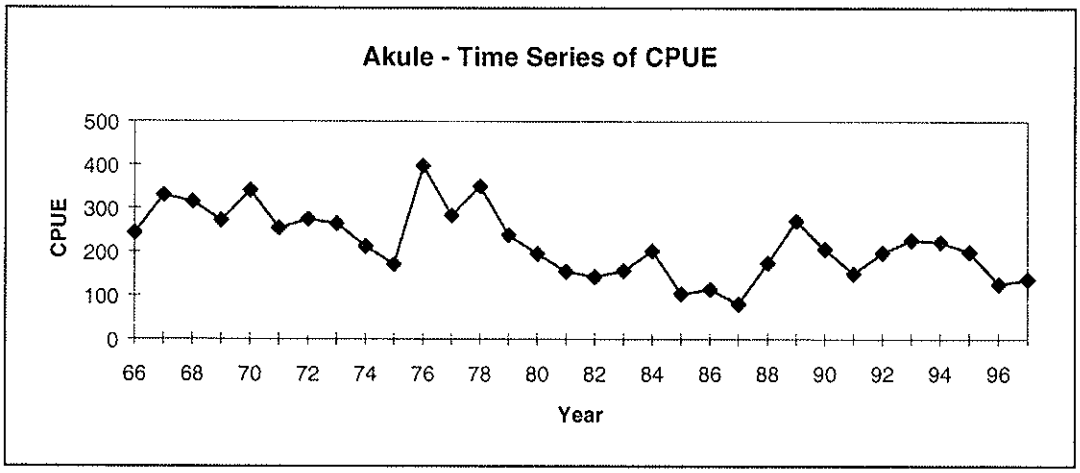

Figure 4. Time Series of Akule *CPUE*

3.4.1.2 Opelu

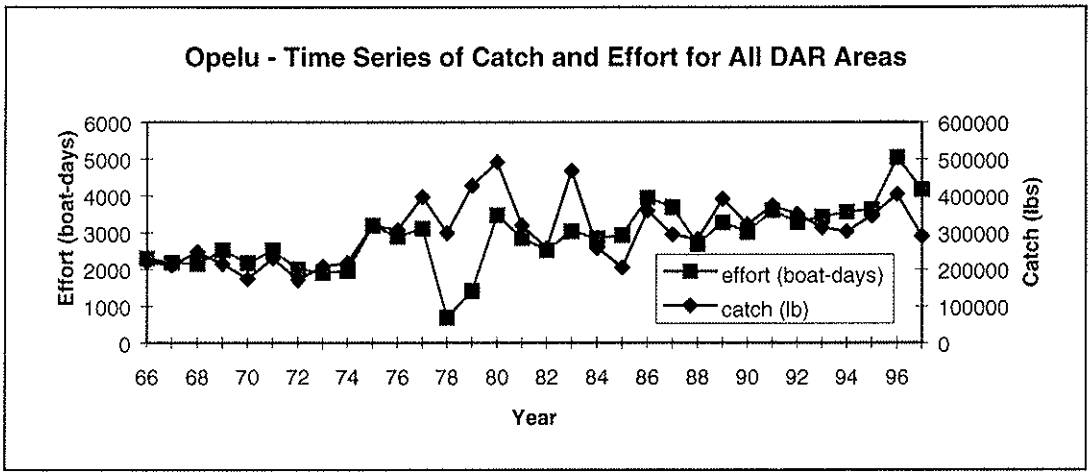

Figure 5. Time Series of Opelu Effort and Catch

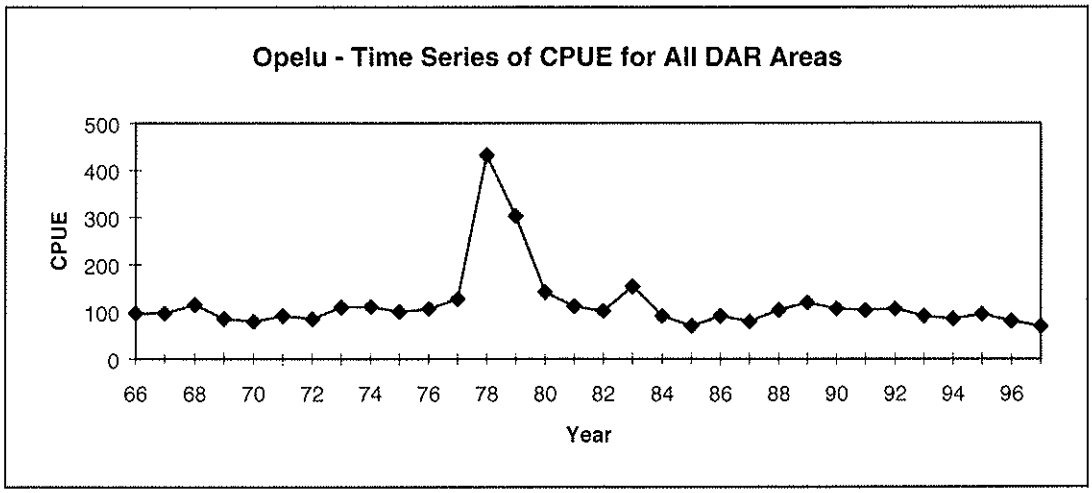

Figure 6. Time Series of Opelu *CPUE*

The opelu *CPUE* time series in Figure 6 shows an extreme peak in the year 1978.

3.4.2 Refined Time Series

Figures 7-12 show time series produced with the following filtered out.

- abnormal *CPUE* days
- days, months, years or licenses of zero

3.4.2.1 Akule

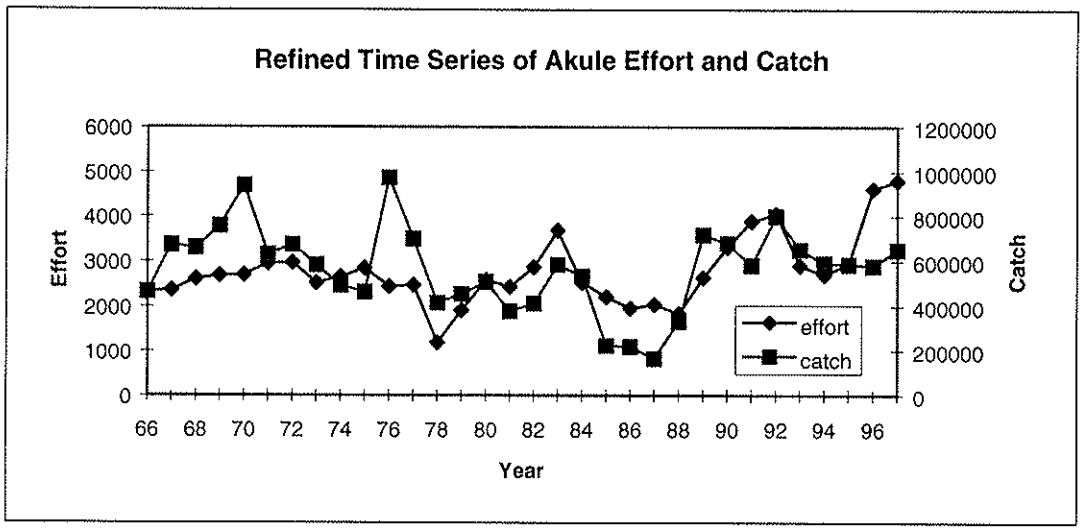

Figure 7. Refined Akule Effort and Catch

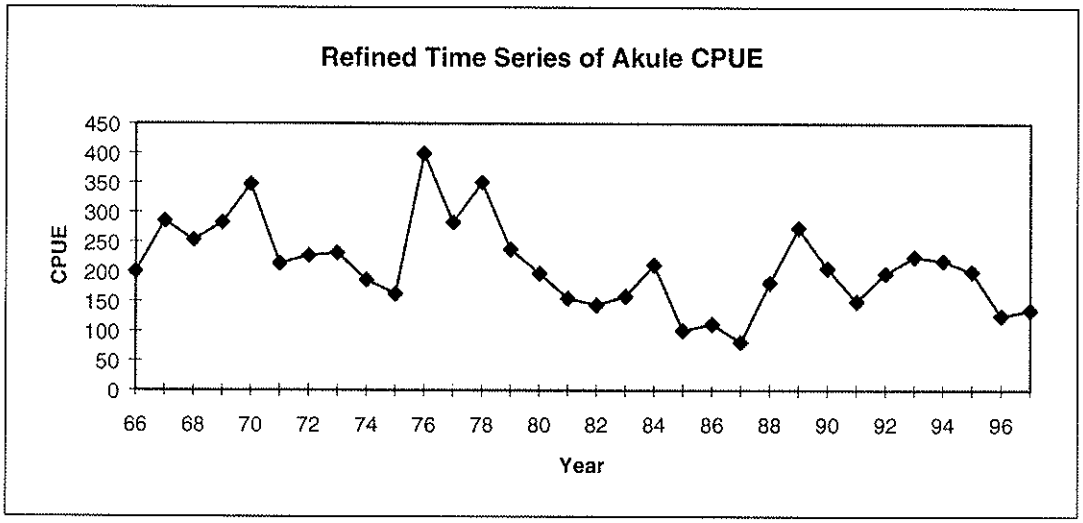

Figure 8. Refined Akule *CPUE*

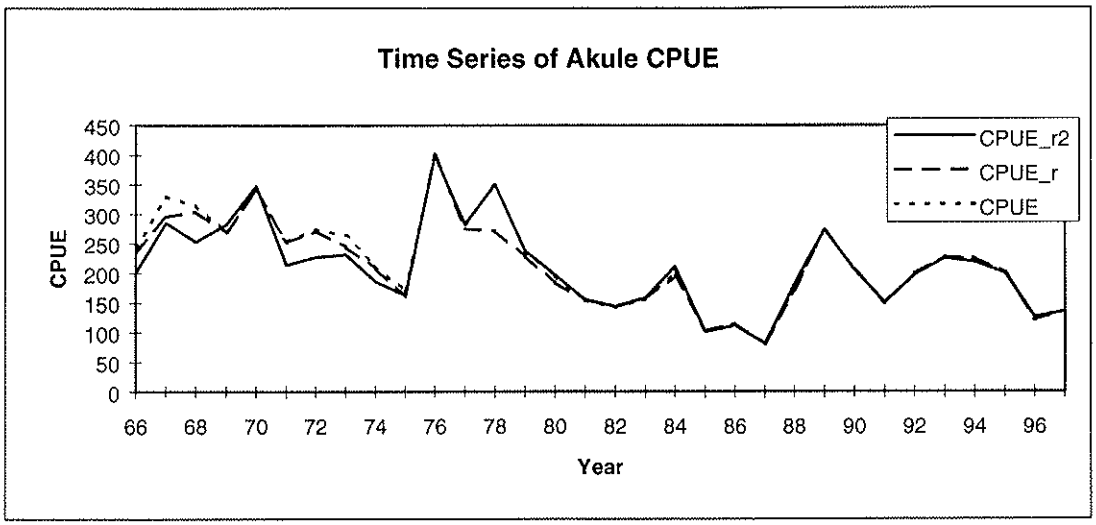

Figure 9. Comparison of Akule *CPUE* Refinements

CPUE	raw
*CPUE*_r	only days of zero, 31 filtered out
*CPUE*_r2	all suspect records filtered out

3.4.2.2 Opelu

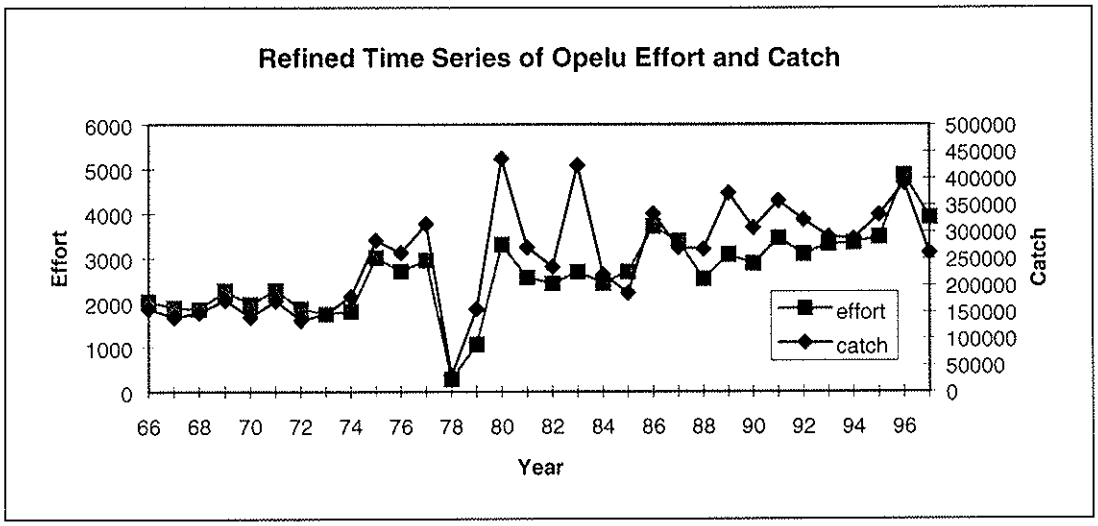

Figure 10. Refined Opelu Effort and Catch

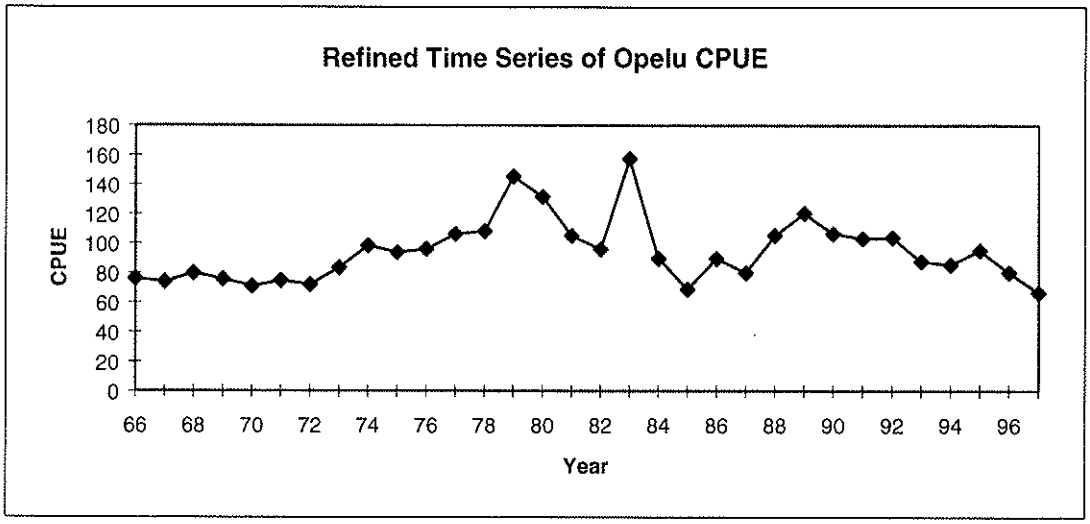

Figure 11. Refined Opelu *CPUE*

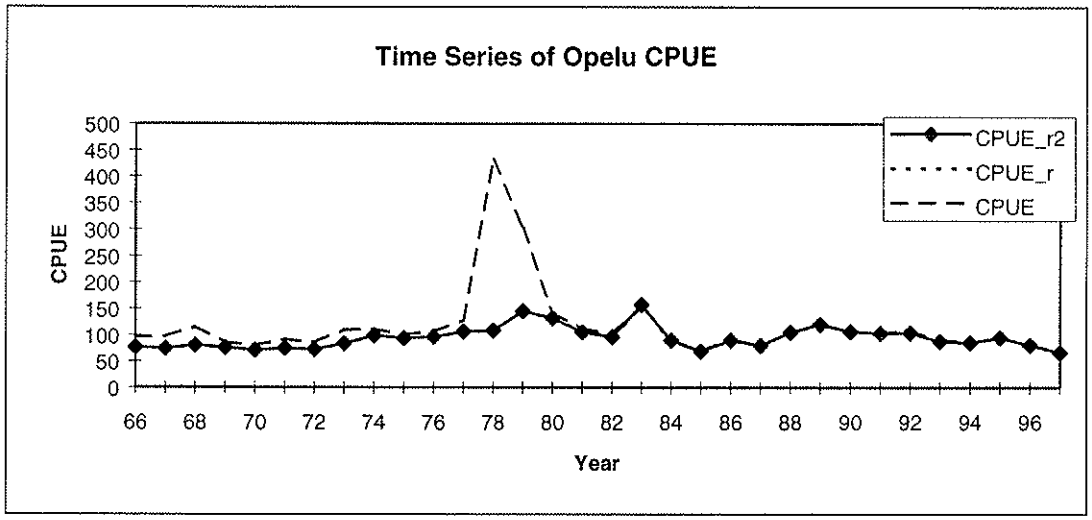

Figure 12. Comparison of Opelu *CPUE* Refinements

CPUE	raw
*CPUE*_r	only days of zero, 30, 31 filtered out
*CPUE*_r2	all suspect records filtered out

Figure 12 illustrates that the only large change is caused by filtering out days zero, 30, and 31 of the month. Other suspect points have very little effect on the time series. Note that the extreme peak for 1978 is removed by the refinement.

3.4.3 Time Series from High Catch Areas

These time series did not differ markedly from those using the full database, so they are not used in further analyses.

3.5 Summary

The DAR database allows the calculation of the basic fishery variables of catch, effort, and *CPUE*. While there is not an explicit measure of effort in the database, it is possible to derive one, the "boat-day," that represents a single day of fishing effort. Various quality control criteria are applied to the data in order to remove sources of bias and error. The resulting refined time series are used in the later stages of this study.

4 DESCRIPTION OF THE AKULE AND OPELU FISHERIES IN THE HAWAIIAN ISLANDS

4.1 Introduction

Akule and opelu fishing has occurred in Hawaii since ancient times, and has undergone considerable changes since the early 20th century. This section describes the fishing methods and the growth in the fisheries during the past 30 years.

4.2 Akule

4.2.1 Methods

Beach seining is one of the traditional akule fishing methods used by the Native Hawaiians. The nets are called hukilau, and are used to take akule schooling very near shore. The proportion of the catch taken with beach seines has declined since about 1920 as other methods have become available. Japanese immigrants introduced *hand lining* in the early 1910's. It is generally conducted at night from small boats using about 5 baited hooks or lures per line. Lights are used to attract plankton, which are the akule's prey, thus attracting schools of akule to the boat (Kawamoto 1973). *Purse seining* uses two boats to surround a school with a net. This method has harvested the largest proportion of akule in the latter half of this century. In the late 1940's, purse seine operations began using spotter planes to search for schools and judge whether the boats should be deployed (Kawamoto 1973).

Commercial fishers take the majority of the akule catch. There is no data on the harvest for subsistence and recreation but these catches are thought to be significant. The primary market for akule is Honolulu, which is the largest city in the state. For this reason, there is higher effort exerted around Oahu and the catch from other islands is generally landed in Honolulu.

4.2.2 Size of the Fishery

The number of boats engaged in the akule fishery has varied considerably during the past 30 years, with an overall increase. The time series in Figures 13 and 14 are obtained by summing the license numbers within each year. Records having a zero or blank in the license field are excluded.

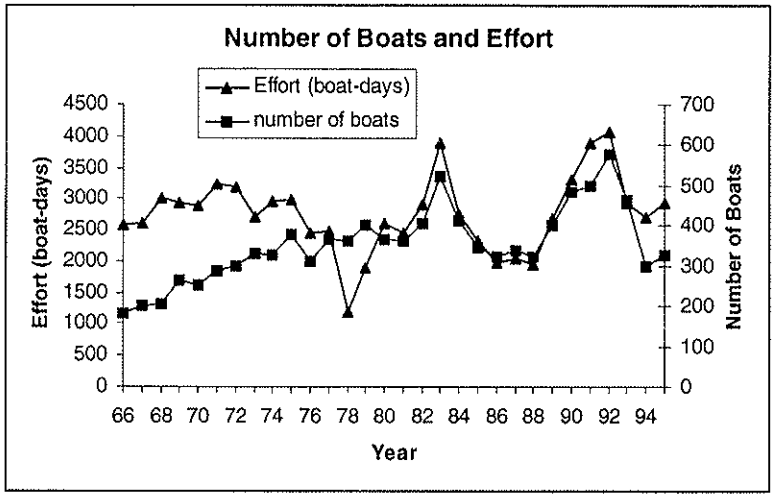

Figure 13. Size of Akule Fishery

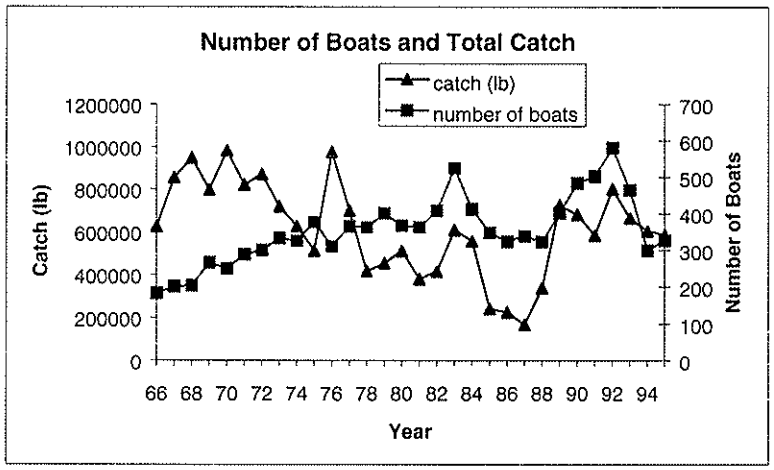

Figure 14. Size of Akule Fishery (2)

In general the number of boats and the effort have changed in parallel, although the first third of the akule fishery shows a higher effort per boat than the remainder. Note that the number of boats using each fishing method cannot be determined because the DAR database does not distinguish between the various kinds of net.

4.2.3 Protection and Management

Since 1929, nets used in akule fishing have been required to have a mesh size greater or equal to 1.5 inches. Since 1968, during the period from July through October, akule less than 8.5 inches total length cannot be netted. This regulation is designed to protect the hahalalu during their recruitment to the adult populations. The Compendium of 1998 Hawaii Fishing Laws regulates akule fishing in *§188-29 nets and traps,* setting the minimum eye size for nets in various gear types and seasons.

4.3 Opelu

4.3.1 Methods and Their Catch Levels

The opelu is taken by hand line and hoop net (Powell 1968). *Hoop netting* is an opelu fishing method developed in Hawaii consisting of a net with a stiff ring at the mouth, deployed vertically from a boat, along with a chum bag and a glass-bottom viewing box. The fisherman observes the operation through a view box and uses the chum bag to attract the school above and into the net. The net is then raised through the school (Gillett 1987). Honolulu is the primary market for opelu.

4.3.2 Size of the Fishery

Figures 15 and 16 show the time series of the number of boats along with effort and catch.

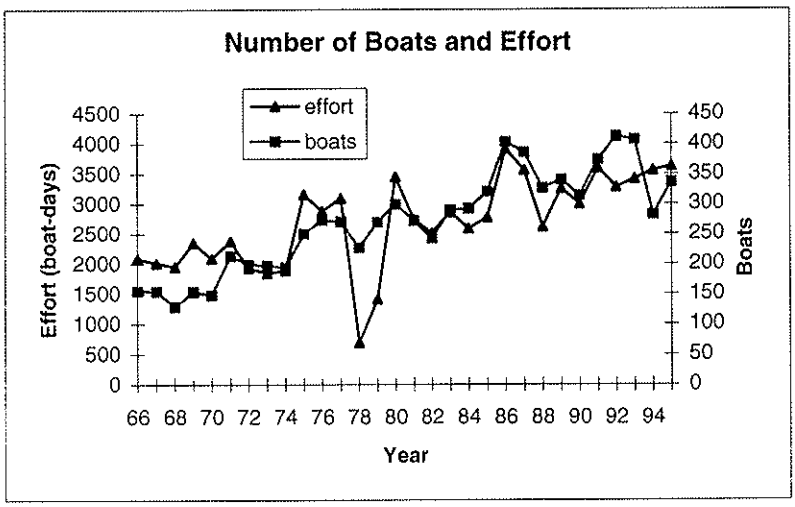

Figure 15. Size of Opelu Fishery

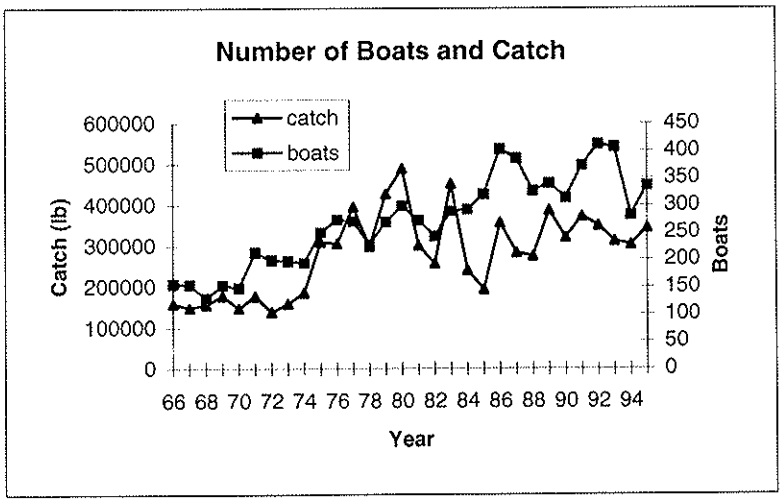

Figure 16. Size of Opelu Fishery (2)

In general, the number of boats and the effort have changed in parallel. Like the akule fishery, the number of boats using each fishing method cannot be determined because the DAR database does not distinguish between the various kinds of net.

4.3.3 Protection and Management

The Compendium of 1998 Hawaii Fishing Laws regulates opelu fishing as follows: *§188-29, Nets and traps,* sets minimum eye sizes for nets as 1-½ inches; *§188-40, Minimum sizes of fish,* sets nine inches as the minimum size; and *§188-46, Opelu fishing regulated,* closes parts of the Kona coast of Hawaii to methods other than hook and line.

4.4 Summary

This chapter describes the methods used in the fisheries for akule and opelu, the regulations that apply, and calculates the changes in the number of boats in the fishery. In general, the number of boats and the effort have changed in parallel, although the first third of the akule fishery shows a higher effort per boat than the remainder.

5 SPATIAL ANALYSIS OF AKULE AND OPELU FISHERIES

5.1 Introduction

5.1.1 Distribution of Catch, Effort and CPUE

Spatial distribution of catch and effort around the main Hawaiian Islands is described in this section. The spatial distribution of catch and effort is important in monitoring a fishery, and in its management and regulation, should this become necessary.

Areas that are important in terms of total yield and *CPUE* are identified in this chapter. Areas with high catch are important regardless of *CPUE* because catching fish is the purpose of the fishery. Areas with high *CPUE* are only important if they also have high catch and contribute significantly to the total yield of the fishery. Areas of high effort are considered important regardless of their *CPUE* because these are the areas of peak activity, and because high effort and low *CPUE* can result from a degraded resource.

5.1.2 Site Fidelity and Localized Depletion

The spatial data is also used to investigate two seemingly divergent, yet interconnected questions: whether the fishing intensity is causing noticeable alteration to natural population dynamics; and the degree of movement the fishes undergo.

In a lightly exploited fishery, the fishing mortality is too small to have a noticeable effect on population dynamics and *CPUE* is unlikely to be strongly reduced. If fishing mortality is significant in relation to natural mortality, *CPUE* will be reduced. If the fish show low site fidelity within the range of a fishery, then any reduction in *CPUE* should occur throughout this range. Alternately, if the fish have high site fidelity within this range, then *CPUE* will be depleted according to the spatial distribution of fishing mortality. Note that low effort areas will not necessarily have high *CPUE*. Low effort areas may be bad fishing spots (low *CPUE*), or good fishing spots that are inaccessible (high *CPUE*). As such, low effort areas will likely show high variability in *CPUE*. Figure 17 shows the expected distribution of points on a plot of *CPUE* vs. effort for low and high site fidelity.

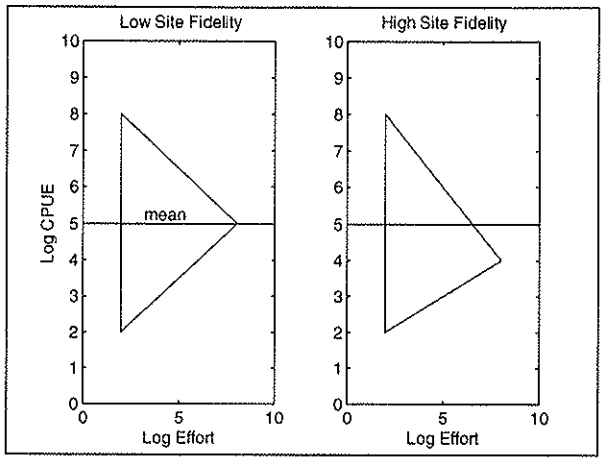

Figure 17. Interpretation of *CPUE*-Effort Distribution The left panel shows the expected shape of the point cloud for a species of low site fidelity. The right panel shows the expected distribution where high site fidelity allows depression of *CPUE* in areas that are intensively fished.

Regardless of site fidelity, the spread of points is expected to decrease as effort increases, because this represents an increase in sampling density. Therefore, the point cloud for both cases is a wedge narrowing towards areas with high effort (i.e., higher sampling density). For a species with low site fidelity, mean *CPUE* is the same for all levels of effort and the wedge is centered on the mean *CPUE*. For a species with high site fidelity, fishing effort can cause local depletion, so *CPUE* is lower in those areas receiving higher effort. Hence the wedge is depressed below the mean *CPUE* as effort increases.

Because site-specific reduction in *CPUE* can only occur with site fidelity, the outcome structure for this analysis is asymmetrical. A positive result indicates that fishing mortality is significant in population dynamics and that site fidelity exists. A negative result allows for the possibility of insignificant fishing mortality, low site fidelity, or both. If an independent method shows that fishing mortality is high, then a negative result for this spatial analysis would indicate low site fidelity.

5.2 Methods

5.2.1 Distribution of Catch, Effort, and CPUE

Maps for effort, catch, and *CPUE* are generated for akule and opelu using the refined data developed in Chapter 3. DAR has divided all waters surrounding the main Hawaiian Islands into areas for use in recording the location of catch and effort. The nearshore waters are divided into two bands—a narrow band bordering the coast and a wider band offshore of this. These areas, and the numbers used to label them, are shown in Figure 18. The databases reference all catches to the areas within these two bands. Because areas vary in size, there is a bias against smaller areas, which is removed by surface-area normalizing. Note that the *CPUE* maps are not surface-area normalized because the areal dimension cancels in the *CPUE* calculation.

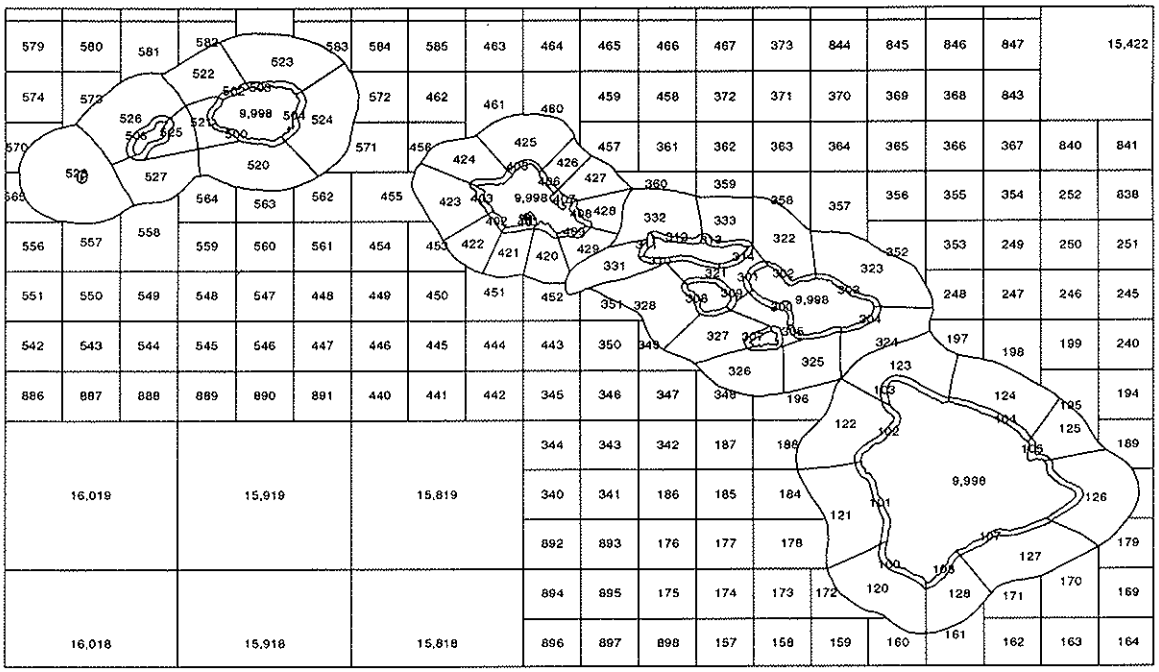

Figure 18. DAR Areas and reference numbers for Hawaiian Waters

Plotting all the spatial data results in maps that show very little variability. The reason for this is that the distribution of the fishery variables in both data sets is heavily skewed to the left (low values), as shown in the histograms in Figures 19 and 20.

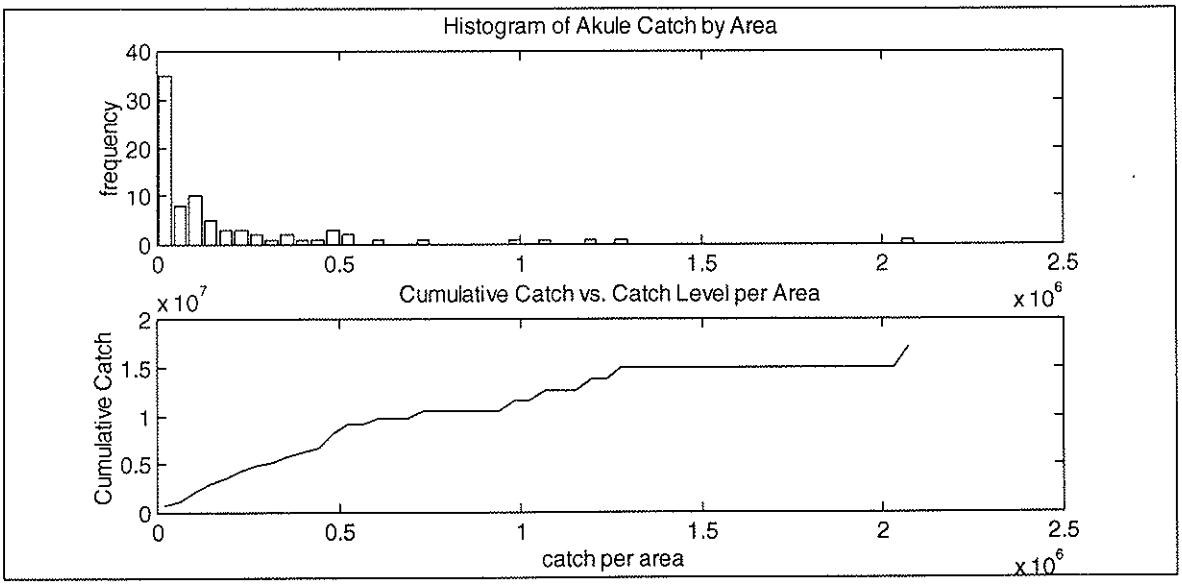

Figure 19. Distribution of Catch (lb) by Area for Akule. The top panel is a histogram showing the strong left-skew of catches. The lower panel shows the cumulative catch achieved at catch bin. Note that a small number of productive areas account for a large portion of the total catch.

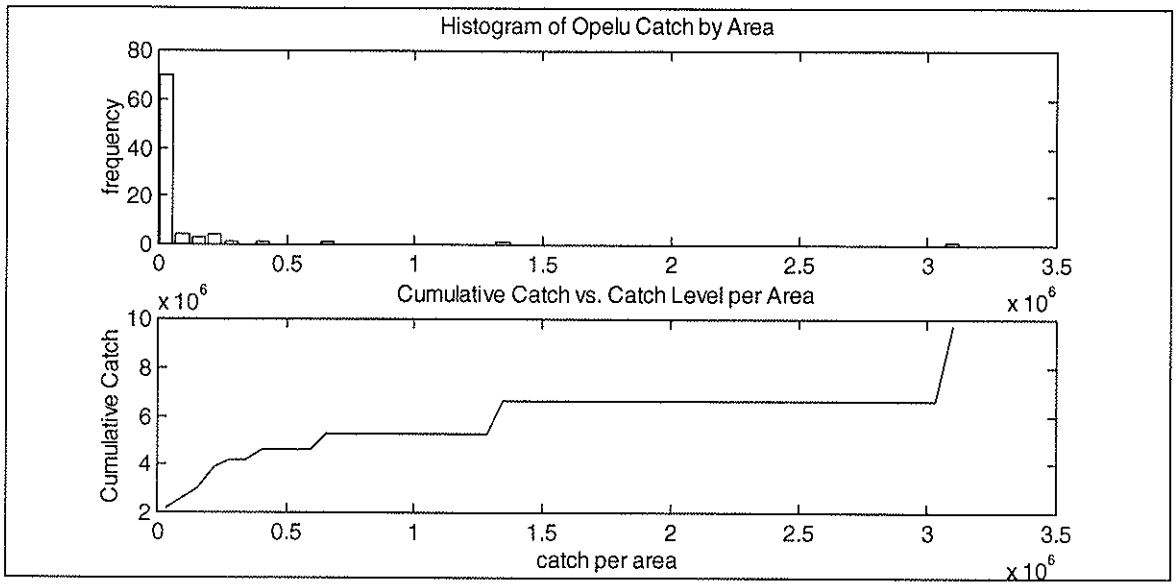

Figure 20. Distribution of Catch (lb) by Area for Opelu. The top panel is a histogram showing the extreme left-skew of catches. The lower panel shows the cumulative catch achieved at catch bin. Note that only two areas account for about half of the total catch.

The areas were placed into 50 bins of equal size. For the akule, the lowest bin contains records with catch below 41,000 lb. per area. For opelu, the lowest bin contains records with catch below 62,550 lb. These areas with very low values impede the display of more useful information for other areas. The cumulative catch plots that accompany the histograms in Figures 19 and 20 show that the smallest catch bins have far more areas than any other, but do not contribute significantly to the catch of the fishery. Therefore, data for these areas is removed in the maps presented here.

5.2.2 Site Fidelity and Localized Depletion

Data for all areas and all catch levels is used in this analysis, because the full range in each variable is desired. To effectively display the highly skewed variables they are Ln-transformed. This yields normal distributions and allows the variables to be standardized (subtract mean, divide by standard deviation). The plots of *CPUE* vs. effort can then be performed. The distribution is compared to the distributions shown in Figure 17 to analyze the effects of effort on local *CPUE*. The *CPUE* in high-effort areas is compared to the *CPUE* in all areas. The definition of high-effort areas is determined by looking for natural breaks in the distribution of the effort data. The significance of any difference between the two mean *CPUE* values is determined using the Student's t test.

5.3 Results

5.3.1 Distribution of Catch, Effort, and CPUE

The following maps (Figures 21–26) present the spatial distribution of effort, catch, and *CPUE* for akule and opelu. The number in brackets after each line in the legend gives the numbers of areas falling within the bin.

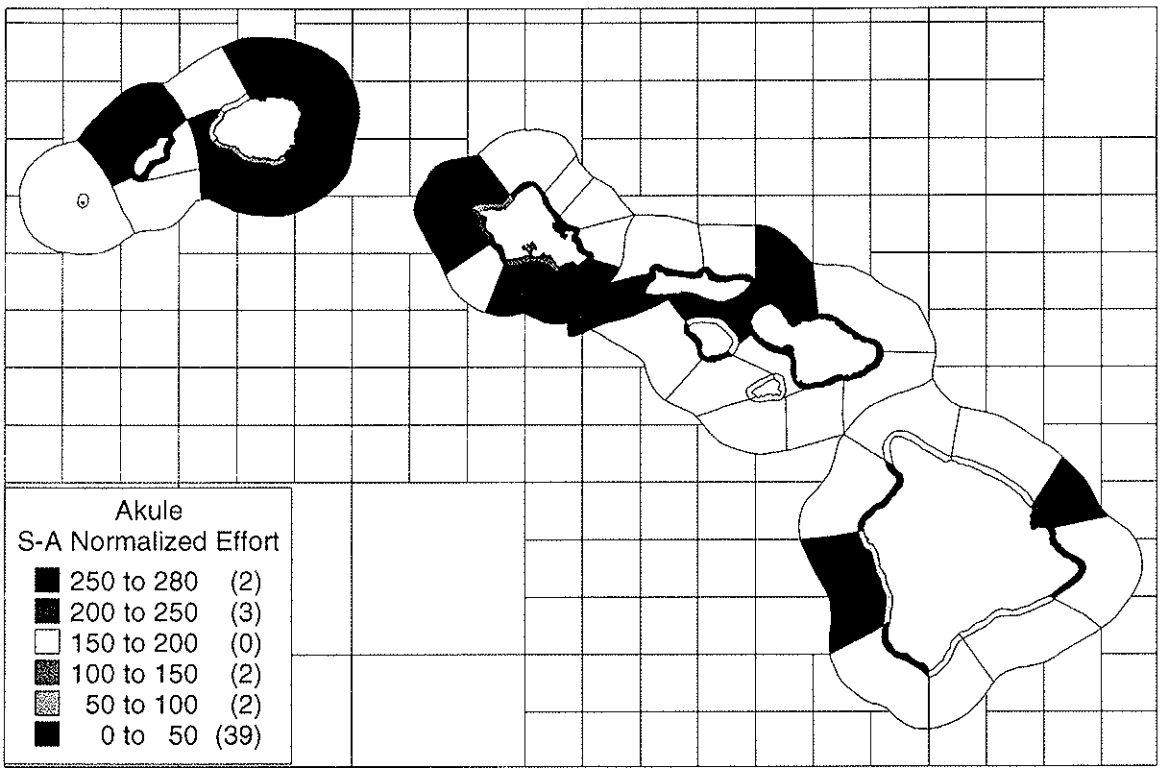

Figure 21. Surface Area—Normalized Akule Effort (boat-days/NM^2)

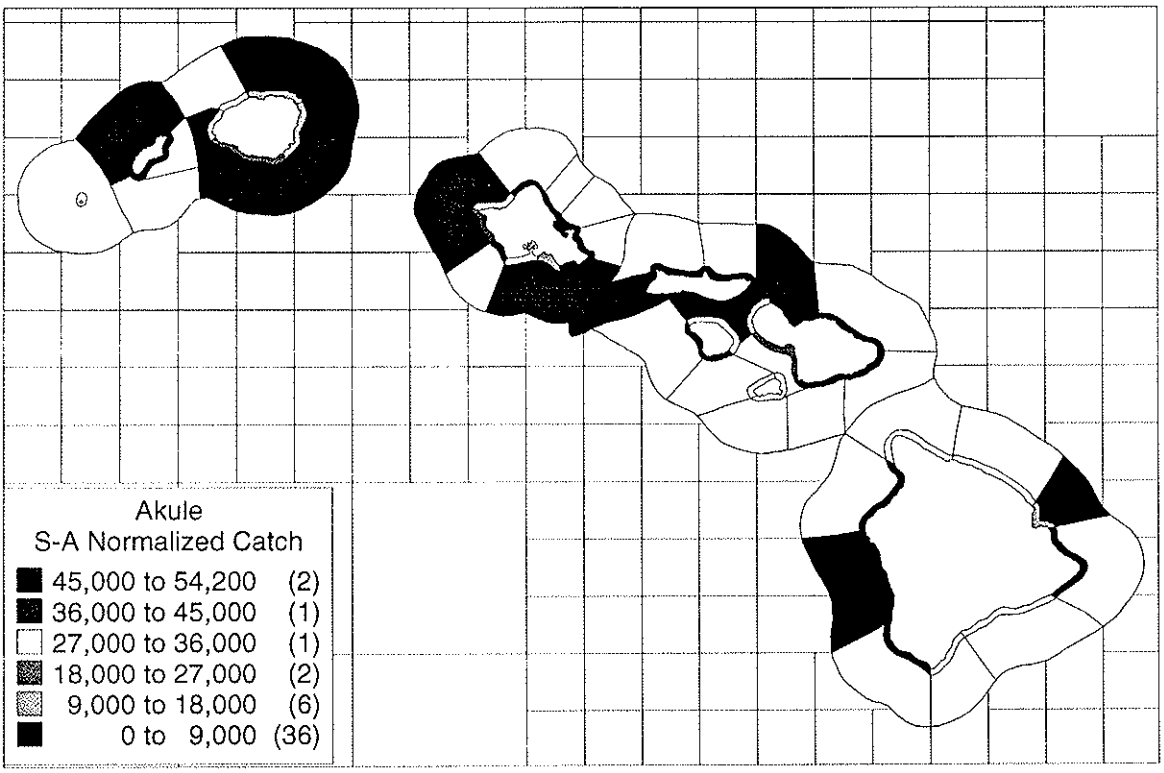

Figure 22. Map of Surface Area—Normalized Akule Catch (lb/NM^2)

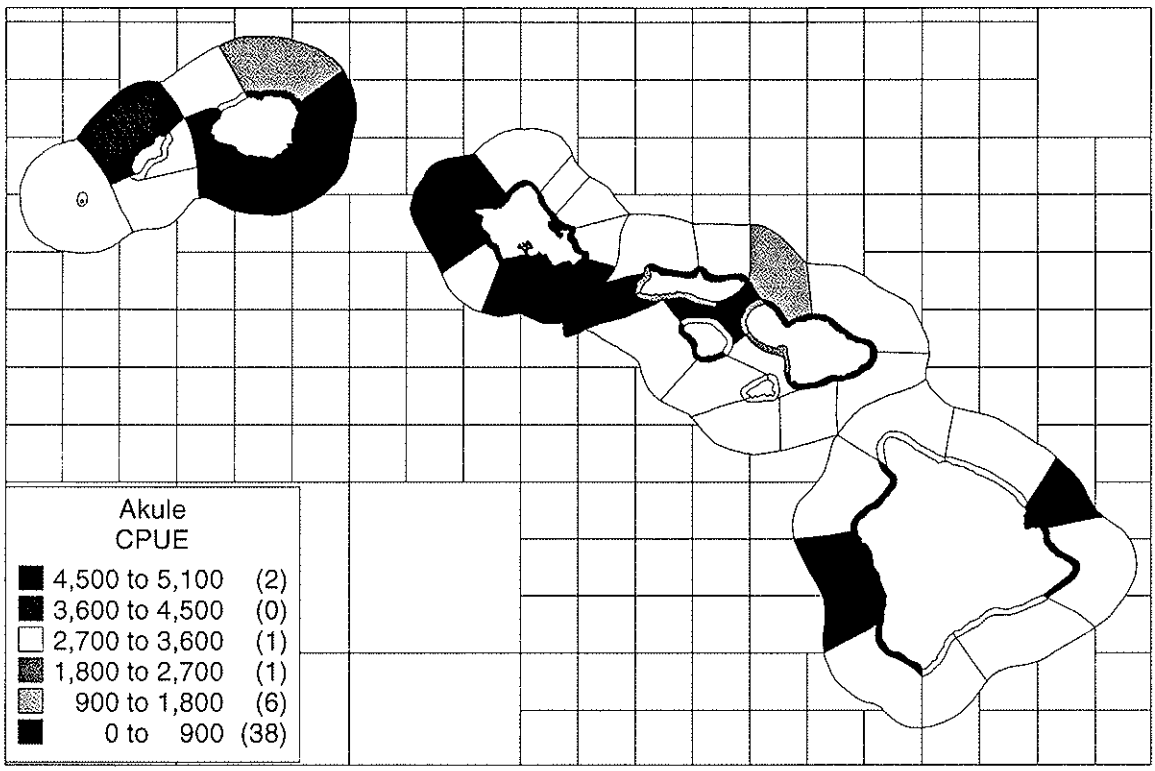

Figure 23. Map of Akule *CPUE* (lb/boat-day)

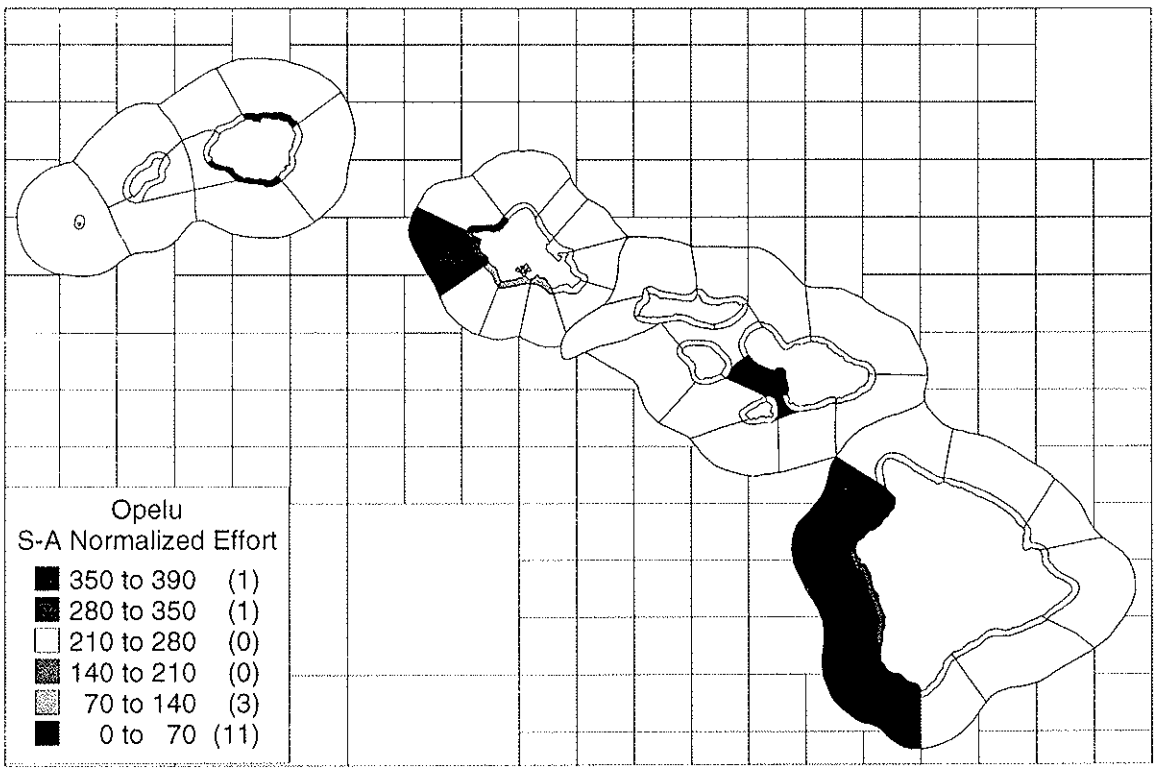

Figure 24. Map of Surface Area—Normalized Opelu Effort (boat-day/NM^2)

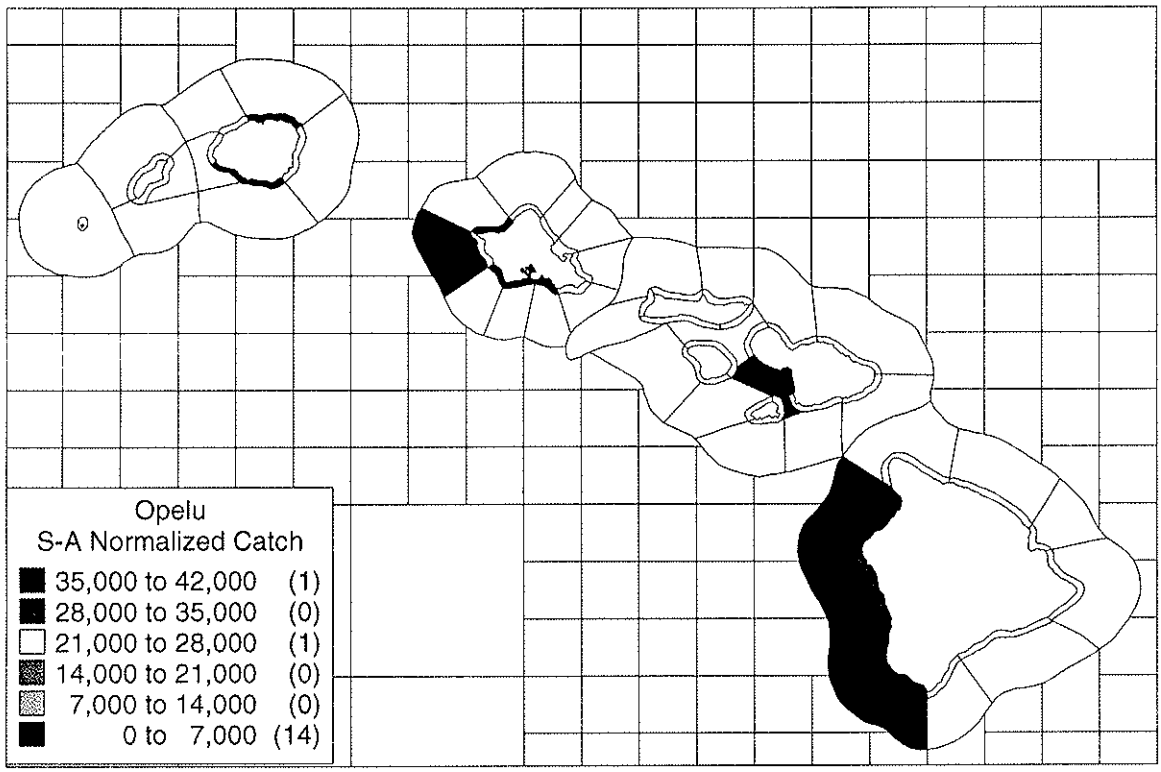

Figure 25. Map of Surface Area—Normalized Opelu Catch (lb/NM^2)

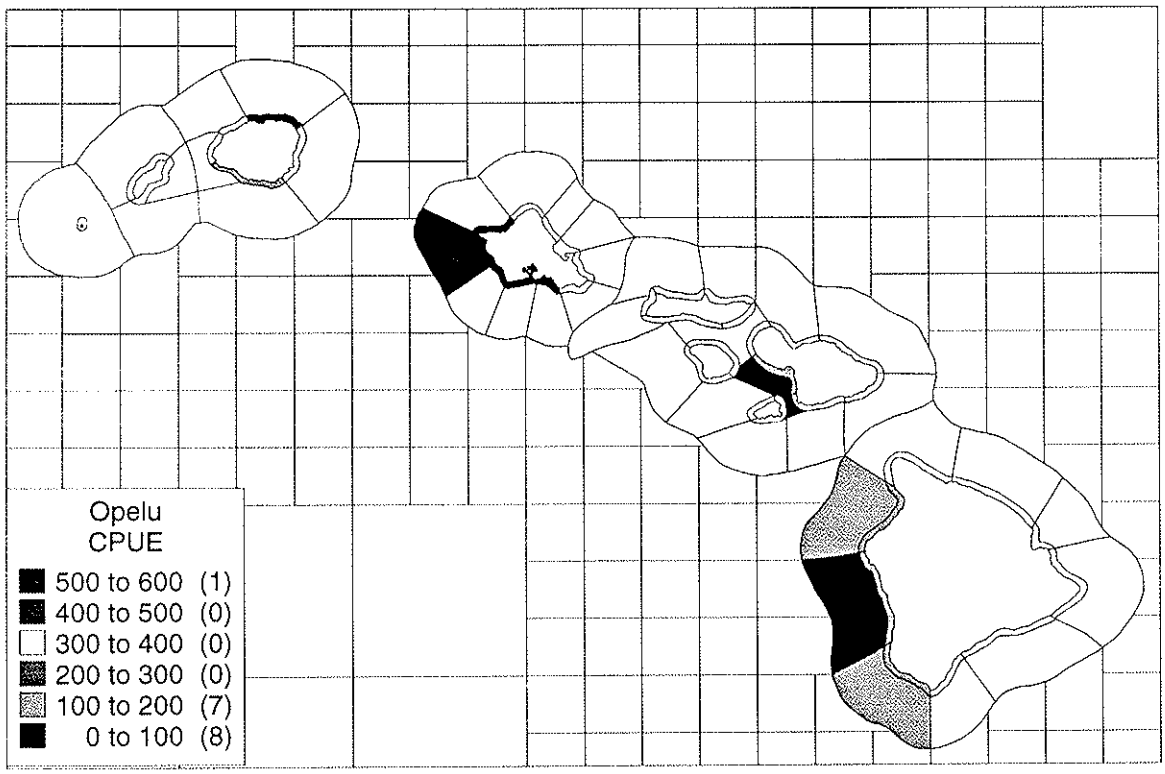

Figure 26. Map of Opelu *CPUE* (lb/boat-day)

The maps allow areas with higher levels of effort, catch, and *CPUE* to be identified. Some areas with high *CPUE* may not be important in the fishery because they have low catch and effort. Therefore, tables 3 and 4 highlight areas with catch and *CPUE* in the upper quartile range.

Table 3. High Catch and *CPUE* Areas for Akule

area		*catch (lb)*	*effort (boat-day)*	*CPUE (lb/boat-day)*
300	Maui	1057162	1089	970.764
310	Molokai	486125	481	1010.655
301	Maui	458869	426	1077.157
506	Niihau	390113	77	5066.403
505	Kauai	337176	121	2786.579
521	Kauai	318162	454	700.7974
305	Maui	260772	109	2392.404

Table 4. High Catch and *CPUE* Areas for Opelu

area		*catch (lb)*	*effort (boat-day)*	*CPUE (lb/boat-day)*
101	Hawaii	3127782	25267	123.7892
121	Hawaii	1333087	14172	94.0648
102	Hawaii	436074	3575	121.9787
100	Hawaii	228475	1791	127.5684
122	Hawaii	196269	1898	103.4083
120	Hawaii	155980	1473	105.8927
300	Maui	129378	1155	112.0156
500	Kauai	129107	899	143.6118
503	Kauai	101494	195	520.4821

5.3.2 Site Fidelity and Local Depletion

5.3.2.1 Akule

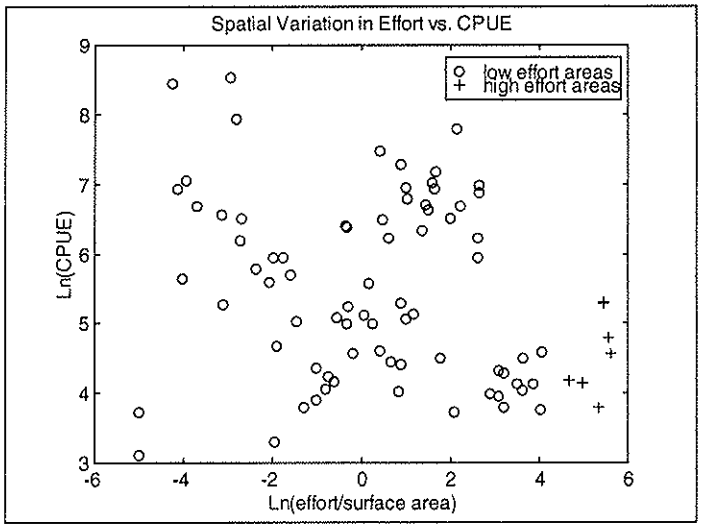

Figure 27. Akule-Effort vs. *CPUE* for All DAR Areas. Compare to Figure 17, right panel. As expected, the point cloud shows highest variability at low effort, and a decrease in CPUE at the highest effort values.

Figure 27 plots *CPUE* against effort for the akule; each point represents a DAR area. Note that the values are surface-area-normalized and Ln-transformed. All DAR areas in the two nearshore bands (see Figure 18) are represented. The wedge shape shows a decrease in *CPUE* variability as effort increases. It also shows a downward trend in *CPUE* towards high values of effort. Therefore, the *CPUE* of high-effort areas is less than the *CPUE* of low-effort areas.

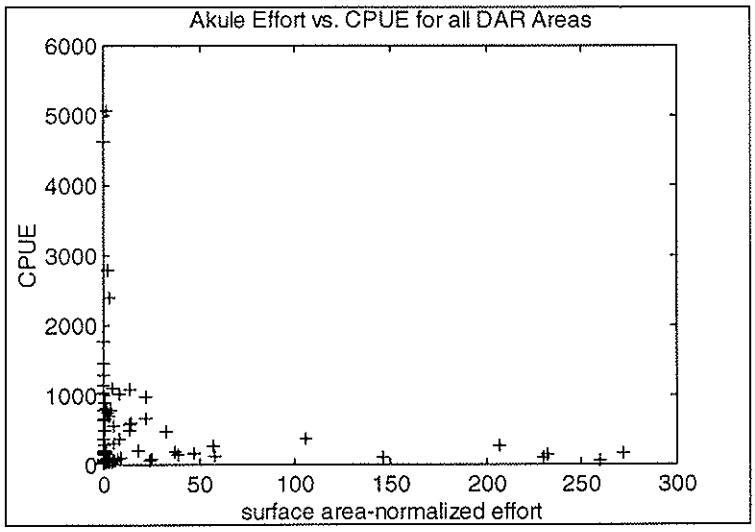

Figure 28. Akule Effort vs. *CPUE* for all DAR Areas. A small number of areas receive much greater effort than the remainder.

Is the difference between these two means significant? Before a formal statistical test can be performed, the meaning of "high-effort" must be determined. Inspection of a plot of effort vs.

CPUE (Figure 28) shows that there is a natural break in the data. Those areas greater than 100 on the effort scale fall outside of the region occupied by the majority of areas.

Given this break in the distribution, these areas are defined as high-effort areas. In Figure 27, this definition is used to distinguish high-effort areas (plus-signs) from low-effort areas (circles). My hypothesis is that the mean *CPUE* of the high-effort areas (μ_{high}) is significantly less than the mean *CPUE* of the remaining low-effort areas (μ_{low}). This hypothesis is stated formally as follows.

$$H0: \mu_{high} = \mu_{low}$$
$$Ha: \mu_{high} < \mu_{low}$$

This hypothesis is tested using a two-sample Student's t procedure. Because the alternative hypothesis is that μ_{high} is greater, a one-sided test is appropriate. The two populations have different variability so a separate variance will be used for μ_{low} and μ_{high}. The test shows that the difference between μ_{low} and μ_{high} is significant at the 99% confidence level (P = 0.0025). The results are summarized in Table 5.

Table 5. Akule CPUE of High and Low Effort Areas

	N	*Mean*	*Standard Deviation*	*Standard Error*
low-effort areas	75	5.500	1.320	0.15
high-effort areas	7	4.584	0.587	0.22
99% CI for μ_{low} - μ_{high}: (0.10, 1.74)				
T-Test: μ_{high}: = μ_{low} (vs. <): T= 3.42 P=0.0025 DF= 12				

5.3.2.2 Opelu

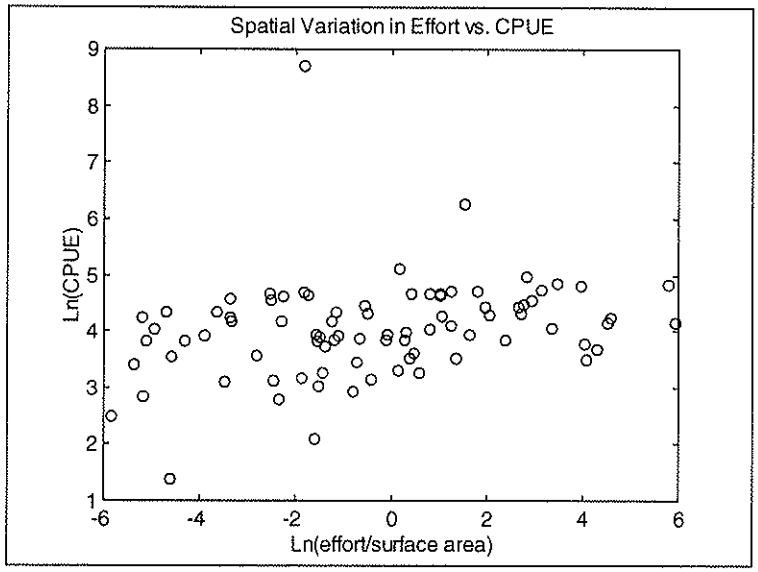

Figure 29. Opelu-Effort vs. *CPUE* for All DAR Areas. Compare to Figure 17, left panel. There is no evidence for depression of CPUE at the highest effort values.

Figure 29 plots *CPUE* against effort for the opelu; each point represents a DAR area. All DAR areas in the two nearshore bands are represented. The opelu data do not form a well-defined wedge pattern, although variability does decrease at higher effort levels.

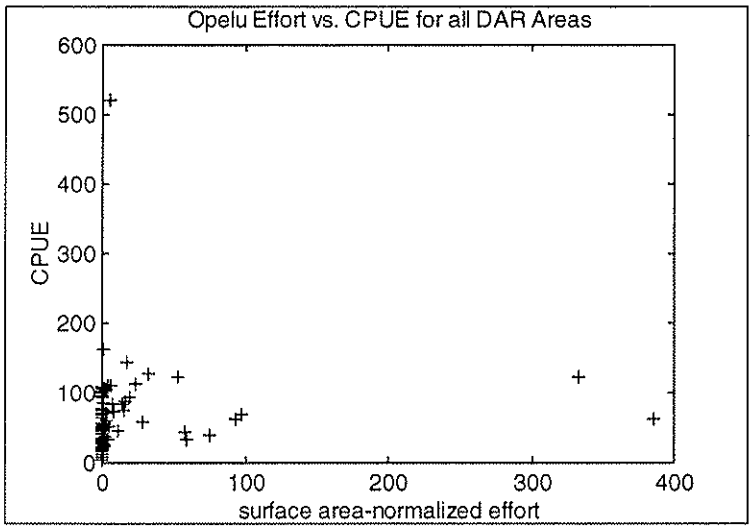

Figure 30. Opelu Effort vs. *CPUE* for all DAR Areas

As with the data for akule, a plot of effort vs. *CPUE* within each DAR area (Figure 30) is inspected for a natural break in the distribution between high-effort areas and all other areas. Note that one area with very high *CPUE* and very low effort is not shown to allow better display of the remaining data. Areas greater than 100 on the effort scale are greatly removed from the region occupied by the remaining points, and are defined as high-effort areas. Using this definition, $\mu_{high} > \mu_{low}$. However, there are only two points in this range so meaningful statistical tests cannot be performed.

5.4 Discussion

5.4.1 Spatial Distribution

The majority of the catch of both species is taken in a small number of areas. The opelu fishery is particularly concentrated, with more than half of the catch for the entire fishery coming from two areas on the Kona coast of Hawaii (areas 101 and 121). This effect is clearly seen in the cumulative catch plot in Figure 20. Area 121 does not show strongly on the catch map because it is a large area and the value is surface-area-normalized.

5.4.2 Site Fidelity and Local Depletion

Site fidelity is of great interest in fisheries management because it strongly affects the kinds of management issues that occur in a fishery. For a species with low site fidelity, an entire stock can be fished despite the effort occurring in only part of its range. Highly migratory and straddling fish stocks can be severely impacted by overfishing in one region or country, to the detriment of fisheries elsewhere. For such a species, fishery closed areas can reduce fishing mortality but cannot afford complete protection to any individual, because the typical adult range will likely exceed the size of the closed area.

For a species with high site fidelity, fishing an entire stock requires fishing over its entire range. Hence, such stocks are often locally depleted where high fishing effort occurs and have normal abundance elsewhere. Such species can be protected with closed areas, which are briefly discussed here. The impacts of fishing on fish stocks are outlined and the amelioration of these impacts by closed areas is discussed as follows.

- *Decreased fish stocks.* Closed areas may export recruited fish into open areas, depending on the typical adult range of a species (Polacheck 1990, DeMartini 1993).
- *Reduced spawning stock.* If fishing decreases the ability of a stock to replenish itself, catch is less than maximum sustainable yield (i.e., an economic loss) and, at some point, the stock will crash due to recruitment failure. Closed areas harbor an "untouchable" spawning stock, and due to the pelagic larval phase of many marine fishes (including akule and opelu), may support recruitment over a considerable region through larval dispersal (Roberts 1997).
- *Removal of large, high-fecundity individuals.* The fecundity of most fishes is proportional to a power function of the size of the female. Therefore, the harvest of larger individuals can have a dramatic effect upon the total supply of eggs. For example, a single 61 cm female red snapper produces the same number of eggs as 212 females of 42 cm each (Birkeland, 1997). For a given species, closed areas generally harbor larger individuals than fished areas (Alcala and Russ 1990).
- *Evolutionary pressure towards smaller individuals.* Fishing removes the most desired fish, generally the biggest. This selects for smaller, earlier maturing fish which, over time, degrades the value of the species to humans. A closed area may harbor individuals that are not subject to this pressure, depending on the movement of individuals across its boundary (DeMartini, 1993, Bohnsack 1996).
- *Decrease in target species, increase in non-target species.* Loss of valuable species makes the system less valuable for fisheries and ultimately leads to the serial depletion of species (Pauly et al. 1998).
- *Coincidence of fishing with natural pressures on a fish stock may cause collapse.* The ocean is dynamic and fish populations go up and down in the absence of fishing. Therefore, a level of fishing that was sustainable yesterday may not be tomorrow. The spawners in a closed area may be able to carry a stock through a protracted period of recruitment failure. In addition to single-species effects, the changes in community structure caused by fishing may cause system-wide effects. The coincidence of high fishing pressure and hurricanes is thought to have precipitated a phase-shift from a coral reef-based to an algal-based system in Jamaica (Hughes 1994). Closed areas with natural community structure can provide a full-community seed stock for the recovery of nearby degraded areas.

These benefits of closed areas will only accrue for species that spend enough time on the inside to gain protection from fishing. The reduction of akule *CPUE* in high effort areas is significant at the 85% confidence level when accounting for variance in both means. Site fidelity for the akule is consistent with the nearshore habitat preference of the akule; tag-recapture experiments around Oahu, Hawaii (Kawamoto 1973); and observations of fishermen that "piles" of akule have regular locations. If the akule shows site fidelity, closed areas may be an effective management tool should this become necessary.

Opelu *CPUE* in high-effort areas is not significantly different from *CPUE* in all areas, indicating low site fidelity, low fishing mortality, or both. The results from modeling (Chapter 6) indicate

that fishing mortality for the opelu is low, and therefore offer no guidance in the interpretation of the opelu's effort-*CPUE* relationship. However, low site fidelity for the opelu is consistent with its habitat, which is more offshore than that of the akule.

5.5 Conclusions

This spatial analysis shows that a relatively small proportion of nearshore waters receive the bulk of fishing effort and produce the bulk of the catch for both the akule and the opelu.

The analysis of *CPUE* with respect to fishing effort shows that akule *CPUE* is reduced in those areas receiving high effort and that opelu *CPUE* is not. This indicates that the akule fishery is significantly affecting population dynamics and that the akule shows site fidelity. The opelu generally lives further offshore than the akule and thus may have lower site fidelity.

Knowledge of site fidelity is critical for the development of spatial management schemes, and is a subject of considerable interest in the literature regarding the use of closed areas for fishery management. Closed areas can effectively protect species with high site fidelity and may be an effective tool for the management of the akule, should this become necessary.

6 MODEL OF POPULATION DYNAMICS

6.1 Introduction

A biomass-dynamic model originally developed by Schaefer (1954) uses the fishery variables developed from the catch and effort databases to estimate biological and fishery parameters for akule and opelu. The term "variable" refers to measured quantities (catch, effort, and *CPUE*) and "parameter" refers to quantities that are estimated from variables.

The Schaefer Model is an ordinary differential equation (ODE) composed of the logistic growth equation, limited by carrying capacity, and coupled with a mortality term that represents fishing. Two versions of the model are developed, one with constant carrying capacity (scalar-k) and one with time-varying carrying capacity (vector-k). The permitted temporal variability of k can be controlled, and three runs are reported at low, medium, and high variability. Both versions of the model employ an equation with semi-implicit time-stepping to prevent chaotic behavior.

The parameters of interest are estimated by time series fitting with maximum likelihood estimation, employing automatic differentiation in a Bayesian statistical framework. Values for the population growth parameter (r) are calculated based on published information. The status of a stock is based upon the biomass in relation to carrying capacity, and the stock-production relationship. The behavior of the model under an idealized fishery confirms its ability to diagnose overfishing, given sufficient contrast in the data. The Bayesian framework allows the use of posterior probability distributions as a means of expressing uncertainty in the results.

6.2 Biomass-Dynamic Modeling

The goal of this exercise is to determine the status of the fisheries for akule and opelu. To do this, we need to know the ecological mechanism of the system and values for parameters in this mechanism that cannot be measured. The mechanism of the fishery is assumed to be that of the Schaefer Model. Estimating relevant parameters necessitates modeling. The database provides effort and catch, allowing biomass-dynamic modeling. The database does not contain catch-at-age data so age-structured models are not an option.

A successful model is one that makes a prediction similar to our observations of nature. When prediction and observation coincide, we can be confident that our mechanism and parameter values are consistent with the data.

A biomass-dynamic model is constructed after Hilborn and Walters (1992). The data required for such models generally include effort, catch, and population growth rate. Length-frequency and catch-at-age data do not exist for these species so age-structured models are not possible.

Hilborn and Walters (1992) provide ODEs for two biomass-dynamic models—the Schaefer model and the Pella-Tomlinson model, summarized in Table 5. The Schaefer model is composed of the logistic growth equation, limited by carrying capacity, and a mortality term that represents fishing. Note that natural mortality is incorporated into carrying capacity in this context. The fishing mortality term, i.e., catch, is calculated with the product of fishing effort and stock biomass. To allow equivalence between catch and biomass, a scale factor (q) is included. This represents the catchability of the stock. By assuming that q is constant, we can use *CPUE* as an index of biomass.

Table 6. Mathematical Forms of Biomass Dynamic Models

Schaefer (Differential equation)	$\frac{dB}{dt} = rB\left(1 - \frac{B}{k}\right) - C$	B	Biomass
		r	Intrinsic rate of population growth
		k	Parameter corresponding to equilibrium stock size
			Catch rate
		C	Time
		t	
	Assumptions:		
	$C = qEB$	E	Fishing effort
		q	Parameter for effectiveness of each unit of effort (catchability)
	$U = C/E = qB$	U	Catch per unit effort
	Properties:		Surplus production (see Section 5.2) and biomass have symmetric relationship; generally there is no information to test this assumption.
Pella-Tomlinson	$\frac{dB}{dt} = rB - \frac{r}{k}B^m - C$	m	Parameter for skew of surplus production-stock size relationship
			All others as in Schaefer model
	Properties:		Allows skew of surplus production-stock size relationship, thereby obviating the Schaefer model assumption of symmetry. Where $m<2 \rightarrow$ left skew; $m>2 \rightarrow$ right skew; $m=2 \rightarrow$ = Schaefer Model
			This model should be used only where skew can be reasonably estimated, which is rarely the case.

The Pella-Tomlinson equation is an extension of the Schaefer equation that allows the stock-production curve to be skewed where such a condition is indicated by data (controlled by the exponent, m). As noted in the above table, the Schaefer equation is equivalent to the Pella-Tomlinson equation where m=2. In practice m can rarely be estimated. No such information is available for the akule and opelu fisheries, hence, the Schaefer model is used.

In order to allow for automatic computations, the ODEs must be written in difference form. The difference form of the Schaefer model is given in Table 6.

Table 7. Difference Form of the Schaefer Model

Schaefer Difference Equation	$B_{t+1} - B_t = rB_t\left(1-\frac{B_t}{k}\right) - C_t$	B_t	Biomass at time t
		C_t	Catch during time t
	where $C_t = qB_tE_t$	E_t	Fishing effort during time t
	Properties:		r, k, q as in Schaefer model
			Where r and qE are low, behavior is the same as for the differential equation Schaefer model. Chaotic behavior occurs for high r-values, "but this is of no real interest in fisheries stock assessment" (Hilborn and Walters 1992: 304) because fish populations do not have high r-values. For an additional margin of safety, a modified form is developed here which prevents this instability.

The logistic equation allows rapid changes in biomass, depending on values for r, and may exhibit chaotic behavior. Therefore, it is necessary to determine the resulting behavior of the Schaefer Model. A number of versions of the Schaefer difference equation are run to determine their numerical stability. The explicit version from the table above allows isolation of the B_{t+1} term on one side,

$$B_{t+1} = B_t + rB_t\left(1-\frac{B_t}{k}\right) - qE_tB_t$$

and it is seen that each value of B depends upon past values of B and E. This version exhibits instability, which is evident when the equation is expressed as

$$B_{t+1} = B_t\left(1+r\left(1-\frac{B_t}{k}\right) - qE_t\right)$$

and if the fishing mortality term qE_t becomes large, the right hand side (RHS) may become negative.

The fully implicit form of the equation

$$B_t = B_{t-1} + rB_t\left(1-\frac{B_t}{k}\right) - qE_tB_t$$

cannot be easily solved, because the value of B at the current time step depends upon values of B and E at the next time step (i.e., in the future). This dependence is evident when the equation is written as

$$B_{t-1} = 1 - r + r\frac{B_t}{k} + qE_tB_t\,.$$

A partially implicit version of the equation is written,

$$B_{t+1} - B_t = rB_t\left(1 - \frac{B_{t+1}}{k}\right) - qE_tB_{t+1}$$

in which B on the RHS is at times t and $t+1$. This change of time dependence is called semi-implicit time-stepping. In this equation, the value of B at the current time step is dependent upon the values of B at the current and previous time step, and E at the previous time step. This equation is numerically stable, and this is evident when it is rewritten as

$$B_{t+1} = \frac{B_t(1+r)}{1 + r\frac{B_t}{k} + qE_t}.$$

Note that the numerator and denominator will both be positive since all the components must individually be positive.

Figure 31 shows the behavior of the logistic portions of the explicit and partially implicit equations (the fishing mortality has been removed).

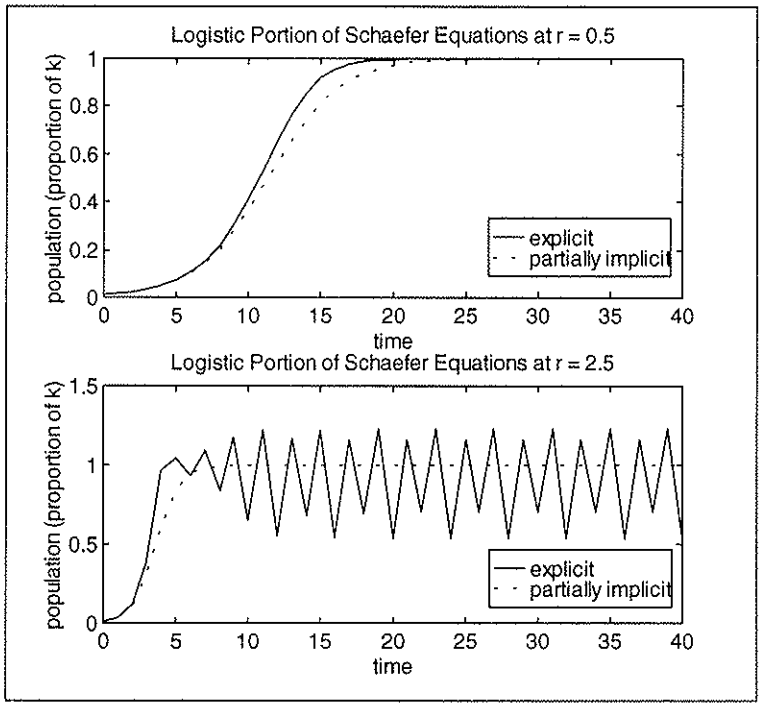

Figure 31. Stability of Explicit and Partially Implicit Logistic Equations. Both versions perform well as low r-values (upper panel). At high r-values the explicit version exhibits chaotic behavior while the partially implicit version remains stable (lower panel).

The top panel shows the behavior for a low value of the growth parameter r. The lower panel shows the behavior for a high value of r. Note that when r is large, the explicit equation is unstable and exhibits chaotic behavior, whereas the partially implicit one is stable. This partially implicit Schaefer equation is used as the scalar-k version of the model (constant carrying capacity). The vector-k version is discussed below under Section 3.3.

6.3 Methods

6.3.1 History of Methods for Fitting a Model to Data

Three methods have generally been used by fishery scientists in fitting biomass-dynamic models to available fishery data: the assumption of equilibrium conditions; transformation of the equations to linear form and using linear regression; and time series fitting (Hilborn and Walters 1992). Of these methods, time series fitting is generally accepted as the most robust (Hilborn and Walters 1992) and is used in the present study. Pella and Tomlinson (1969) first developed this method. Initial values of relevant parameters are chosen and the model is used to predict the data. The initial parameters are changed and the model is run again. Based on the differences between runs, the initial parameters are adjusted to achieve a closer fit, and so on, until the best estimates are found through iteration.

6.3.2 Methods for Time Series Fitting

6.3.2.1 Maximum Likelihood Estimation

Time series fitting is accomplished in this study by using maximum likelihood estimation (MLE). MLE is described in many sources, such as Brownlee (1965). In order to estimate values for the model parameters (r, q, K, B_0) based on the closest fit of the model to the data, we minimize an objective function that is based on the deviation of the predictions away from the data. The function should be appropriate to the distribution of the estimates around the data. For instance, where the estimates are normally distributed around the data, a sum-of-squares function is appropriate. This likelihood function, L, is then a dome-shaped function of the parameter(s), θ. To find the maximum value of L, the partial derivative of L by θ is set to zero (the slope of the function is zero at the maximum). In practice it is easier to use the logarithm of L. Where there is more than one parameter, the partial derivatives of L by each θ are set to zero, thus

$$\frac{\partial \log L}{\partial \theta_1} = \frac{\partial \log L}{\partial \theta_2} = \cdots = \frac{\partial \log L}{\partial \theta_i} = 0.$$

If there was a single parameter, θ, then the likelihood function would be searching for the peak on a line. If there were two parameters, it would be searching for the peak on a curved surface. Because there are more than two parameters, the likelihood function is searching for the peak of an n-dimensional space. In this case there is no simple visual analogy such as a line or surface.

For simple likelihood functions, analytic, closed form expressions for θ_i are feasible. For the more elaborate likelihood functions encountered in the present study, numerical searches are necessary. The software AD Model Builder (Fournier 1996, 1999) is used for maximum likelihood estimation. This software uses a quasi-Newtonian numerical minimization algorithm with analytical gradients determined by automatic differentiation (see Section 3.2). The objective function that is minimized by this algorithm is chosen to reflect the relevant quantities

from the core equation, in this case, the partially implicit Schaefer equation. For the scalar-k version of the model, the objective function is

$$\log L = \sum \left(\log(\hat{C}) - \log(C) \right)^2$$

where $\hat{C}$ is the predicted catch and C is the observed catch (data). The sum-of-squares term decreases the function as deviations between $\hat{C}$ and C decrease, thereby leading to a closer fit as $\log L$ is minimized.

The objective function for the vector-k model is discussed in Section 3.3.

6.3.2.2 Automatic Differentiation

In order to determine the gradient of the partial derivatives, software packages such as AD Model Builder employ a technique called automatic differentiation. The basic principles behind automatic differentiation are simply the fundamental rules of differential calculus. Using the chain rule, the program takes the function and breaks it up into simpler components that can be differentiated, then recombines the results into the solution to the original equation (Iri 1991).

6.3.3 Statistical Framework—A Bayesian Approach

6.3.3.1 Background

The models used in this project use a Bayesian approach, which differs from the classical approach in that pre-existing knowledge or impressions of a parameter are quantified in the analysis. Unknown parameters are replaced by known distributions for those parameters. Based on this prior knowledge, and the available data, the statistical test determines how likely we are to observe a given parameter value (Schmitt 1969). Formally, the pre-existing information is represented in the prior probability distributions, the new information (data) is represented in the likelihoods, and the combined result of the two is contained in the posterior distributions (O'Hagan 1994).

Cause and effect are placed on the same conceptual level—both are treated as random variables, which allows inversion in our statistical tests (Robert 1994). In effect, the causative factors are treated as if they were caused by our observations. If a cause, C, gives rise to an observed effect, O, then the probability distribution of the effect is given by

$$O = C + \epsilon$$

where ϵ is an error term. The Bayesian makes the conceptual leap that an identical distribution describes the probability distribution of the cause, given the observation of the effect,

$$C = O + \epsilon$$

(Robert 1994).

Classical statisticians object to Bayesian techniques, arguing that unknown parameters cannot be considered to be random variables as they do not arise from controlled experiments (O'Hagan 1994). Bayesians counter that, while it is true that a causative parameter does not arise out of a random experiment, treating it as a random variable is often the best available method of incorporating the available (or unavailable) information regarding the parameter (Robert 1994). Note that the "answer" is not a single value for the parameter of interest, but a probability distribution of values for the parameter. The peak of the distribution is generally the value used, and the shape of the distribution is a measure of confidence in this value. A narrow distribution indicates high confidence, and vice versa. The probability distribution for a parameter is often referred to as a likelihood profile.

6.3.3.2 Variable Carrying Capacity

It is widely accepted that the ocean is a dynamic system and can cause variations in carrying capacity for many organisms. Therefore, we know that assuming constant k is likely to lead to error. Assuming that carrying capacity does vary, in an unknown way, is a more reasonable assumption (for further discussion see Fournier 1996).

This method does not attempt to directly determine the changes that carrying capacity has undergone. Rather, it allows us to quantitatively explore the questions "If k does vary, then what variation would yield the *CPUE* time series we observed, and how close would the model's fit be?" This is the basis for the second version of the Schaefer Model, in which carrying capacity varies in time.

The equation used in the scalar-k model is modified by making k a time-dependent variable, as follows

$$B_{t+1} = B_t + rB_t\left(1-\frac{B_{t+1}}{k_t}\right) - qE_tB_{t+1}$$

where k is defined as

$$k_{t+1} = k_t \cdot \exp(\eta_t)$$

and η is $N(0,\sigma_\eta)$, a normally distributed random variable with mean zero. σ_η is set to allow at least the desired degree of variability in k. The model chooses values of η for each time step such that the predicted catches approach the actual catches. In this way, the model generates a time series of carrying capacity that improves the fit of predicted catch to observed catch (and is not based upon empirical evidence of changes in k).

The form of the objective function ensures that k is not completely free to vary because variation in k adds to the function, thereby penalizing such variation. Variation in k occurs only until the benefit of improved fit is equal to the cost of variation in k. This balance is achieved with the following objective function.

$$\log L = \sum\left[\log(\hat{C}) - \log(C)\right]^2 + w\sum\eta^2$$

This function is the same one that is used for the scalar-k model plus $w\Sigma\eta^2$, a penalty term that increases log L as σ_η increases. In order to improve the fit of $\hat{C}$ to C, the model varies η, causing k to change; the nature of this change is adjusted so that $\Sigma[\log(C')—\log(C)]^2$ decreases.

The weighting term, w, is used to vary the size of the penalty so that the variation of k can be adjusted. Note that this model has a special case—when w is large $\Sigma\eta^2$ is small and the variation in k is minimal, so the model approaches the scalar-k model.

6.4 Model Inputs

6.4.1 Effort and Catch Data

For both akule and opelu, the refined time series discussed in Chapter 3 are used. For the test case using an idealized fishery, monotonically increasing effort and a dome-shaped catch function are used, which cause monotonically decreasing *CPUE*. Constant carrying capacity is assumed. This scenario is an idealized form of the classic unmanaged fishery, with effort increasing through time and catch increasing then decreasing as the stock becomes overfished. This test case allows the behavior of the model to be observed in a scenario with a known outcome.

6.4.2 Values for the Population Growth Parameter, r

The model does not estimate r with confidence, so values are calculated using a published method and data from published sources. For the test cases, the value calculated for the akule is used.

Sullivan (1991) provides an empirical equation for r as a function of K, based on estimated r and K values for 44 stocks of commercially exploited fishes. This equation requires K and the asymptotic weight, W_∞, as inputs. Asymptotic length, L_∞, can be converted to W_∞ with the relationship $W = a \cdot L^b$ where a and b are empirical constants. Weight is in grams and length is in centimeters.

6.4.2.1 Akule

There are no published r-values for akule other than Kawamoto (1973). Nineteen published sources provided K-values for the akule (compiled in Froese and Pauly 1998). W_∞ is available only from Kawamoto (1973). Other sources provide L_∞. Using this information and the relationships stated above yields an r-value of 1.94/year.

6.4.2.2 Opelu

Yamaguchi (1953) and two sources in Froese and Pauly (1998) give K-values for the opelu. L_∞ is provided in Gushiken (1983) and two sources in Froese and Pauly (1998). Using this information and the equation of Sullivan (1991) yields an r-value of 1.86/year.

6.5 Model Outputs and Interpretation

The model provides estimates for various biological and fishery parameters, from which additional parameters can be calculated. The model also provides various outputs quantifying its

performance and the closeness of fit achieved. These parameters are used to assess the condition of a stock. They can be used to infer whether the stock is overfished, optimally exploited, or could support increased fishing.

6.5.1 Model Performance Diagnostics

The model measures the closeness of fit by the size of the objective function, which is defined in Section 3.2.1. Note that the functions are different for the scalar-*k* and vector-*k* models, in that the term which penalized variation in *k* for the vector-*k* model is absent (i.e., zero) for the scalar-*k* model. Hence, while the vector-*k* objective function has an extra term adding to its size, the ability of *k* to vary may allow the function value to be lower than that for the scalar-*k* model, indicating a closer fit.

6.5.2 Stock Assessment Diagnostics

6.5.2.1 Biological and Fishery Parameters

The model estimates catchability, *q*, carrying capacity, *k* (or initial carrying capacity k_0), and initial biomass B_0. Using these values and effort and catch from the data, the model calculates predicted catch, biomass, carrying capacity, and maximum sustainable yield. For the vector-*k* models, the penalty weight for variation in *k* affects the outputs. The results are presented with three penalty weights and the confidence plots are presented for the medium penalty.

The most useful of these outputs are *MSY* and the ratio B/B_{MSY}. When catch exceeds *MSY*, overfishing is occurring. When B/B_{MSY} has a value of one, the stock is optimally exploited and sustainable yield (or surplus production) is at its maximum. When B/B_{MSY} is less than one, the sustainable yield is less than it could be and the fishery is not in its most productive state. When this is the case, allowing the stock to recover will result in higher yields.

The conditions of a stock can be visualized when the surplus production is plotted against the stock biomass. The surplus production (analogous to sustainable yield) is the amount of fish produced during a time step over and above what is required to maintain the population level. The following equation is used to calculate surplus production.

$$\text{surplus production}_{(i+1)} = \text{biomass}_{(i+1)} - \text{biomass}_{(i)} + \text{catch}_{(i+1)}$$

Figure 32 shows how the stock-production relationship is interpreted.

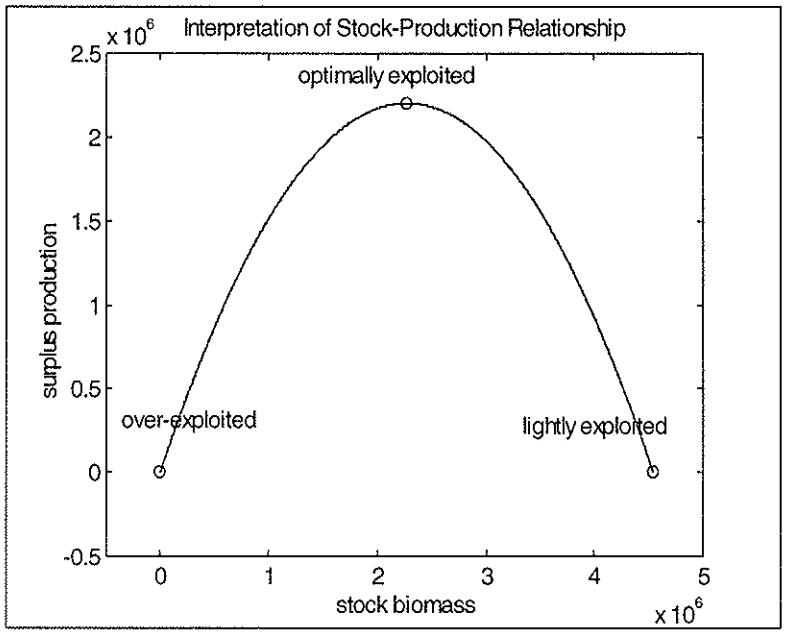

Figure 32. Interpretation of Stock-Production Relationship

There are three theoretically known points for the stock-production curve. The production is zero at a biomass of zero, and when biomass has reached carrying capacity. *MSY* occurs at a biomass of k/2. A line can be fit to the three known points (0,0), (k,0) and (k/2,MSY) and is referred to as the theoretical stock-production curve. Note that a given surplus production can occur at two levels of biomass either side of B_{MSY}. The right end of the curve shows the stock at *k* (i.e., saturated) where the environmental limits to growth have been reached and the surplus production is zero. As fishing moves the stock left from *k* to k/2, fish are released from *k*-limitation so they grow and reproduce faster, and higher surplus production is achieved. The peak of the curve occurs at a biomass of k/2 and represents the optimal balance between the release from *k*-limitation and the loss of spawning stock. As fishing moves the stock left from k/2 towards zero, the benefit of release from *k*-limitation is eclipsed by the detriment of decreased spawning stock, and surplus production declines. In general, recruitment failure will cause a population crash before fishing reduces the biomass to zero.

Note that a trend in *CPUE* is not enough to assess the condition of a stock. *CPUE* will decrease as biomass decreases, but this only becomes a problem when biomass is less that k/2. Similarly, *CPUE* may be constant but if biomass is less than k/2 the stock is overfished, and allowing recovery would enable higher sustainable yields. The outputs of the Schaefer Model allow the theoretical curve for the stock in question to be plotted, as well as the actual stock-production values for each time. The distribution of these points in relation to the theoretical curve allows the condition of the stock to be assessed. Fisheries with low contrast in the data will show points that are narrowly distributed on a stock-production plot. The position of the point cloud allows the status of the stock to be assessed. Note, however, that high confidence in the results is only possible where high contrast exists in the data.

6.5.2.2 Confidence

Confidence in the vector parameters is assessed by the width of their one standard deviation bounds, a measure of spread requiring normality, which was confirmed. Confidence in the scalar parameters is assessed by plotting their likelihood profiles, as discussed in Section 3.3. The sum-of-squares likelihood function used in this model requires the distribution of the estimates around the data to be normal, which was confirmed.

6.6 Results

The results are presented as time series plots for the vector parameters and number values for the scalar parameters. In addition to the direct outputs of the models, surplus production is calculated and used to analyze the stock-production relationship for each stock. For the vector-k models, variation in k is controlled by a penalty factor, discussed in Section 3.3. Results are provided for low, medium, and high penalty levels (except for the test case, which is provided at a single penalty level). Confidence in the results is assessed with various quantitative measures of statistical spread.

6.6.1 Test Case for Scalar-k Model

The test case uses data concocted to represent an idealized fishery, having monotonically increasing effort and a dome-shaped catch function, which cause monotonically decreasing *CPUE*. Constant carrying capacity is assumed.

Figure 33 shows that the model incurs minor error—the B/B_{MSY} ratio equals one when the predicted catch is maximized (year 78), prior to the time the actual catch is maximized (year 82). However, the trend of the B/B_{MSY} ratio correctly describes the trend of the fishery. It actually adds a precautionary margin because it prematurely indicates the point at which *MSY* is reached. A precautionary approach to management has been advocated widely (e.g., Gordon 1994).

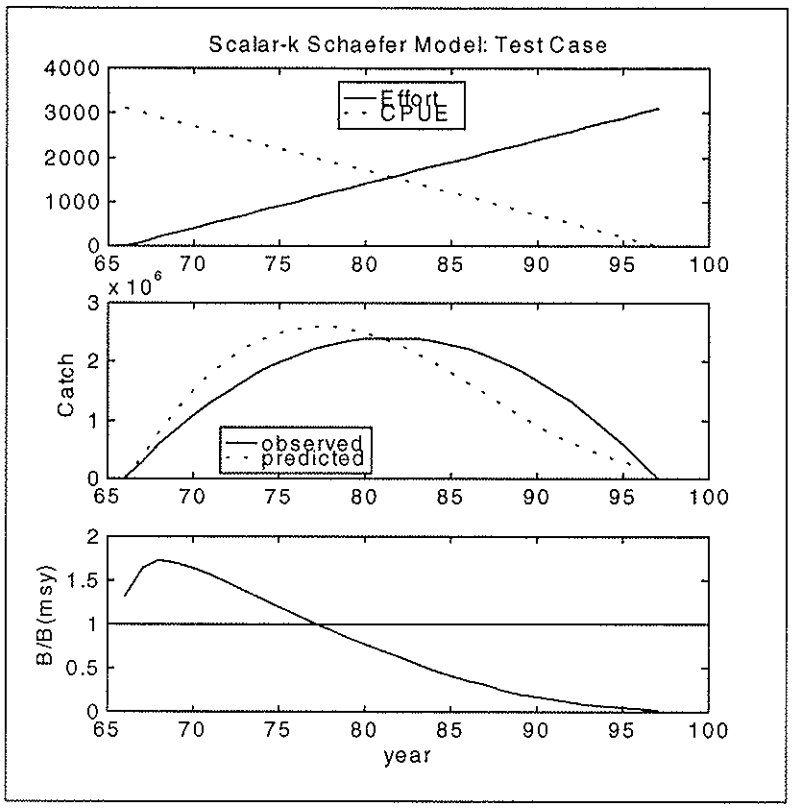

Figure 33. Scalar-*k* Model Input and Output Time Series for Test Case. The model successfully diagnoses a troubled fishery in this test (see text for details).

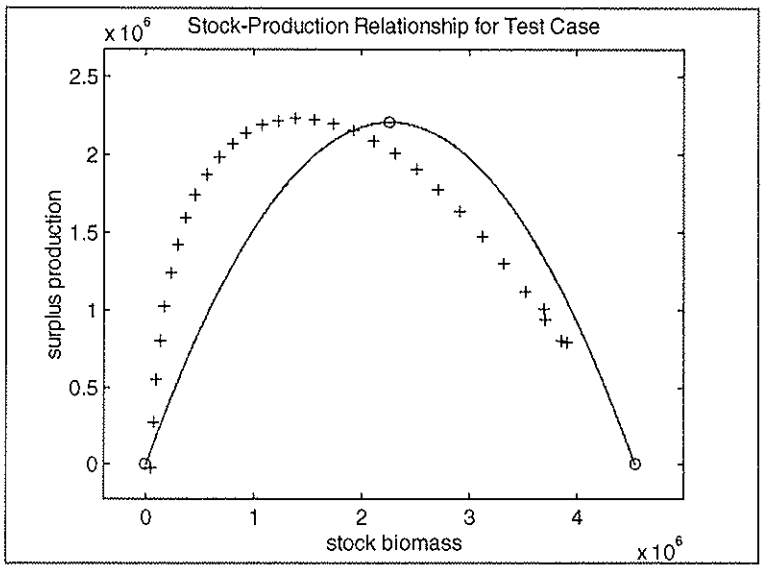

Figure 34. Scalar-*k* Model—Stock-Production Relationship for Test Case. The full range of values shows the transition of the stock from pristine (right) to extinct (left).

Figure 34 shows that the stock-production prediction is skewed from the theoretical relationship because there is error in the model output, as discussed above. However, the error is small, and the form of the relationship is shown. Note that almost the full range of possible values is

represented because the concocted data follow the fishery from a pristine to an extinct condition. This high contrast in the data, along with the absence of noise in the input data, leads to the high confidence levels as reflected in Figures 35-37.

In Figure 35, the one standard deviation bounds on the output time series are very narrow, reflecting the confidence that results from a high contrast data set.

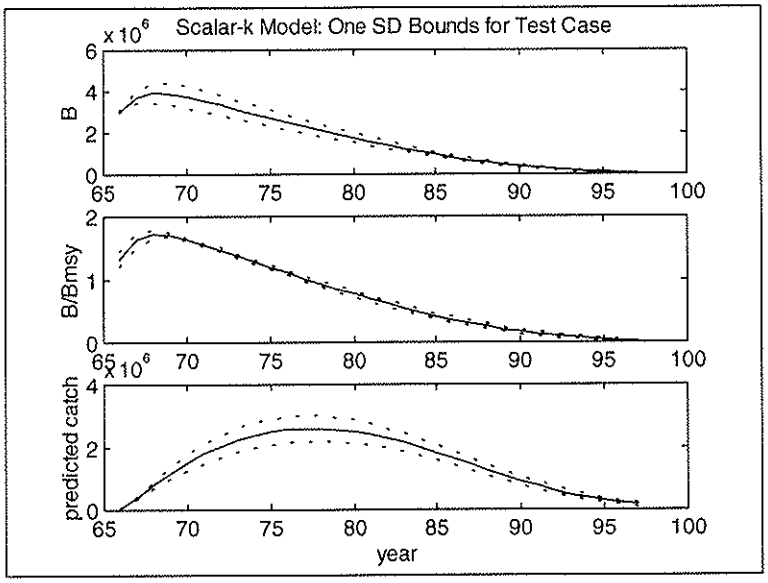

Figure 35. Scalar-*k* Model Output Time Series with 1-SD Bounds. The narrow 1SD bounds indicate high confidence in the results.

Figures 36 and 37 show that the likelihood profiles for the scalar parameters are narrow. Note that *MSY* is a direct function of *k*, and does not have an independent likelihood profile.

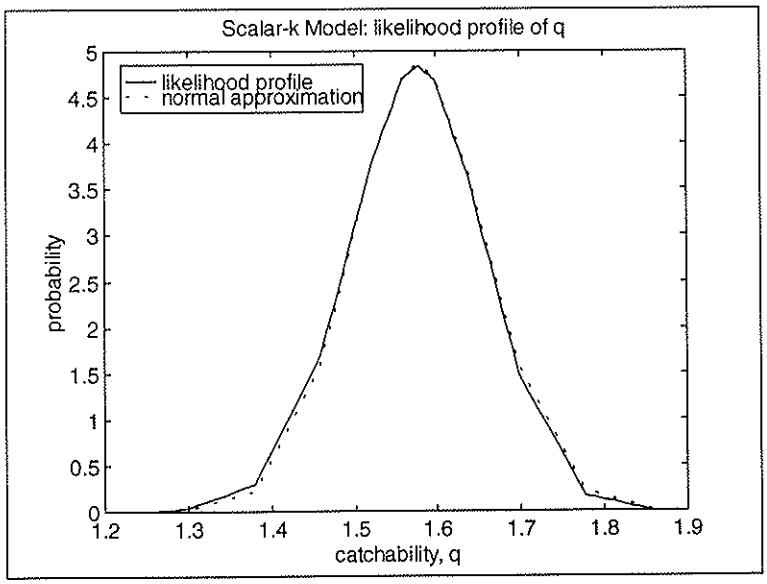

Figure 36. Scalar-*k* Model—Likelihood Profile of 'q' for Test Case

significance level	lower bound	upper bound
0.9	1.42446	1.72157
0.95	1.4017	1.75106
0.975	1.37893	1.77376

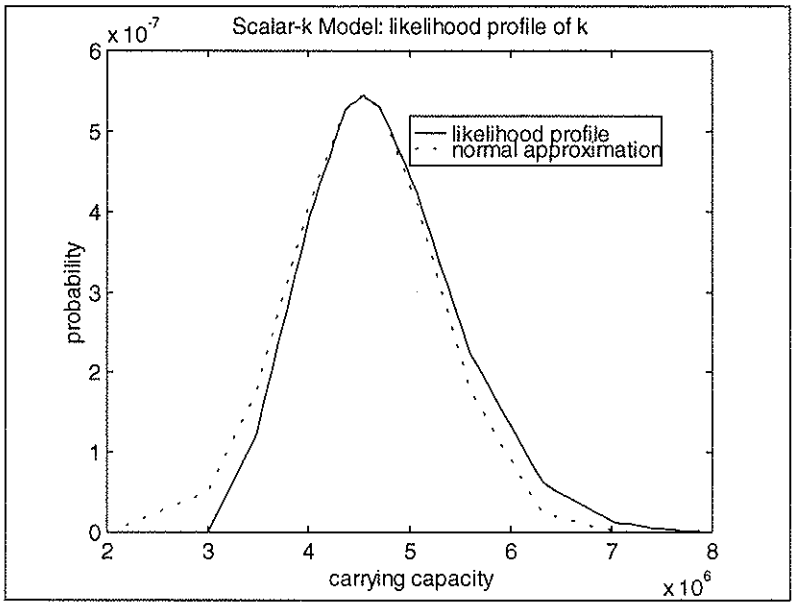

Figure 37. Scalar-*k* Model—Likelihood Profile of 'k' for Test Case

significance level	lower bound	upper bound
0.9	3.47771e+06	6.0315e+06
0.95	3.27298e+06	6.28835e+06
0.975	3.13649e+06	6.56115e+06

6.6.2 Test Case for Vector-k Model

The same idealized fishery input data are used as a test case for the vector-*k* version of the model.

Figure 38 shows that the vector-*k* model incurs some errors, but it correctly identifies the trend of the fishery. However, the time at which *MSY* is indicated (year 84) is after the time when observed catch is maximized (year 82), meaning the model is late in diagnosing overfishing. This error arises because the model's ability to vary *k* is used to explain a portion of the variability in *CPUE*. Because the test case uses a constant *k*, this leads to error and the variation of *k* masks the reduction in *CPUE* for a period.

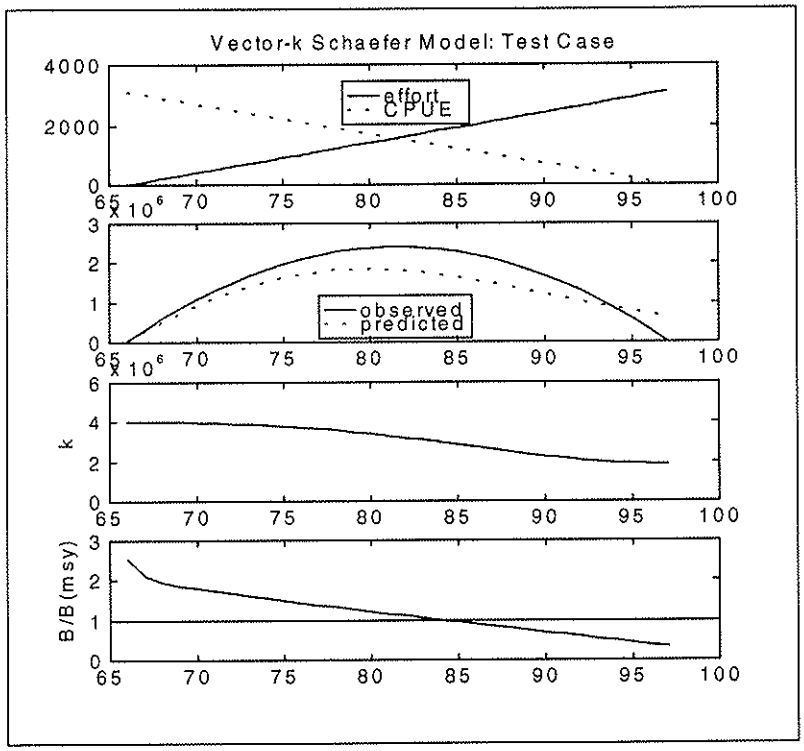

Figure 38. Vector-*k* Model Input and Output Time Series for Test Case. The model successfully diagnoses a troubled fishery in this test, although the variation in *k* causes a lag (see text for details).

Figure 39, the theoretical stock-production relationship, is based upon the mean values for the three known points in a variable-*k* scenario. The predicted *k* falls below the output points that are based upon the actual *k* at the time. This relationship also shows that the data have high contrast, with the full relationship represented in the output values. This leads to low variance in the outputs, as shown in Figures 40 and 41.

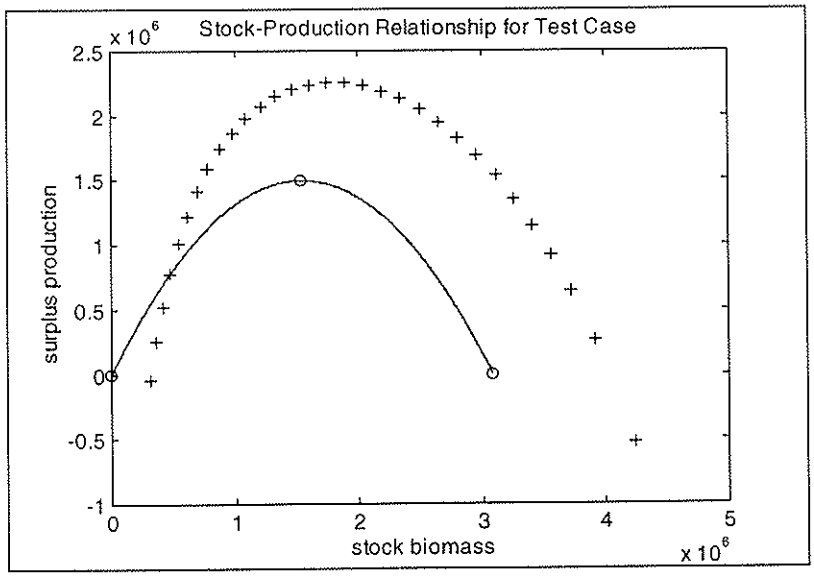

Figure 39. Vector-*k* Model—Stock-Production Relationship for Test Case. The full range of values indicates the transition of the stock from pristine (right) to extinct (left).

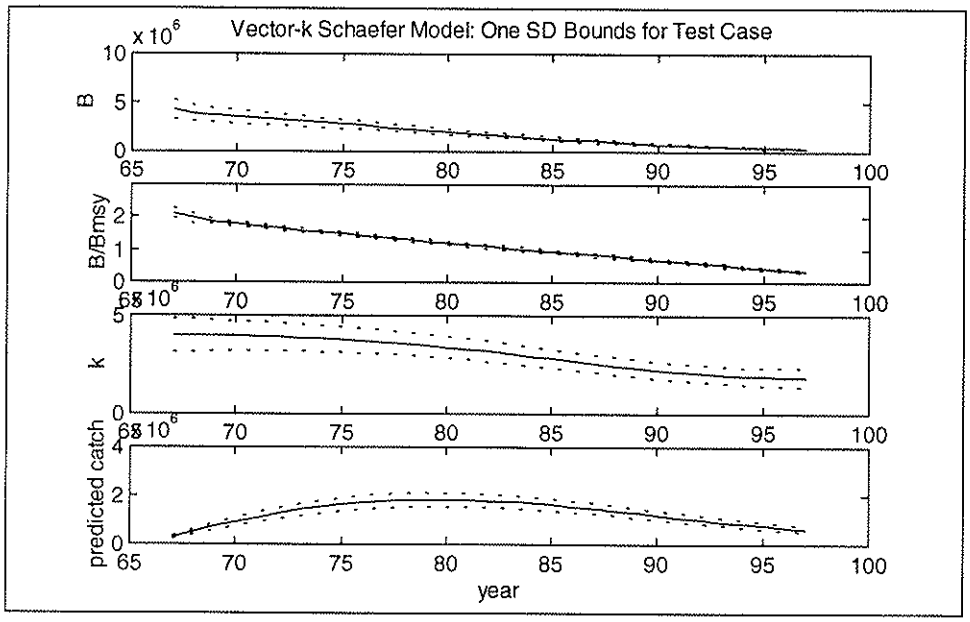

Figure 40. Vector-*k* Model—Output Time Series with 1-SD Bounds for Test Case. The narrow 1SD bounds indicate high confidence in the results.

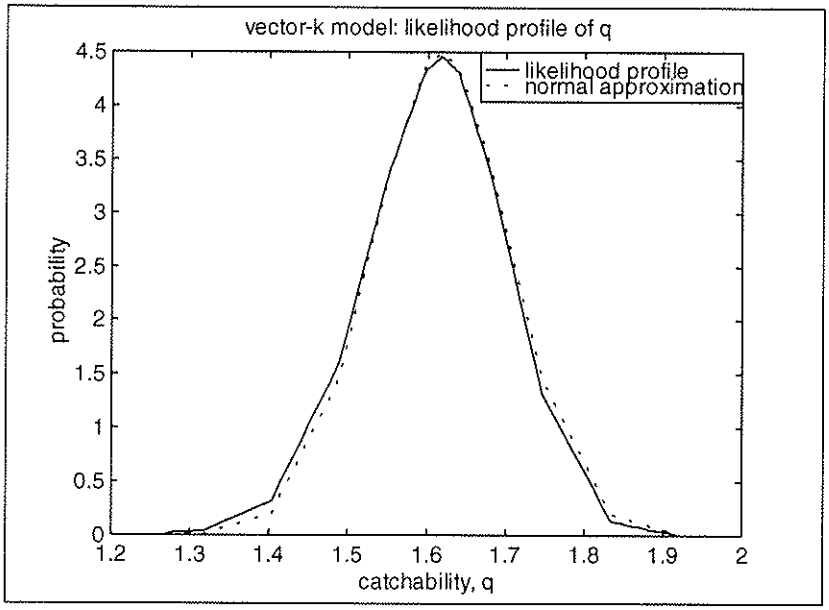

Figure 41. Vector-*k* Model—Likelihood Profile of 'q' for Test Case

significance level	lower bound	upper bound
0.9	1.44817	1.7719
0.95	1.41534	1.79651
0.975	1.39046	1.82423

As for the scalar-*k* test case, confidence in the results of the vector-*k* model is high, due to the high contrast data set.

6.6.3 Scalar-k Model for Akule

6.6.3.1 Output Parameters

Figure 42 shows that biomass gradually declined with moderate inter-annual variations, but has always been above B_{MSY}. Predicted catch approximately follows the shape of observed catch, indicating a moderate fit. Note that some of the y-axes have been truncated to allow higher resolution.

Objective function value, log L = 3.836
Catchability, q = 0.562
Carrying capacity, k = 1.343e+06
Maximum sustainable yield, MSY = 651292

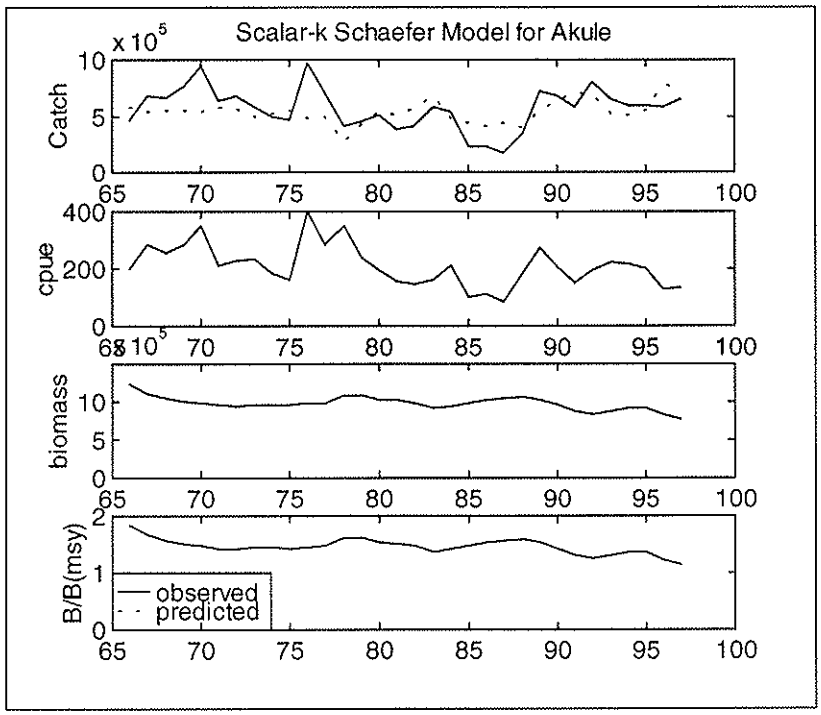

Figure 42. Scalar-*k* Model Input and Output Time Series for Akule. Trends are interpreted in the text. Compared to the test case, the variability is higher and contrast is lower.

The theoretical stock-production curve for the stock is shown in Figure 43. The point cluster is about 1/3 of the way from *MSY* to the zero exploitation point, indicating that the stock is exploited somewhat below *MSY*. Note that some of the points are higher on the surplus production axis than the theoretical *MSY* point, indicating overfishing during these times. The surplus production is calculated as described in Section 5.3. In Figure 43, the calculated points are marked with pluses and the theoretically known points, based upon data from the model, are marked with circles (see Section 5.3 for details).

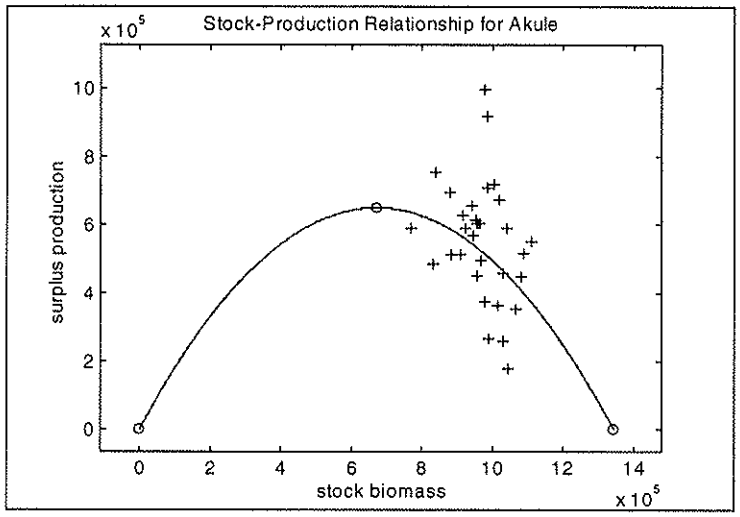

Figure 43. Scalar-*k* Model—Stock-Production Relationship for Akule. The points lie in a small portion of the graph, showing the low contrast in the data, which leads to low confidence.

6.6.3.2 Confidence in Results

Figure 44 shows that B is not well determined in the data because the 1 SD bound is below zero for part of the time series. B/B_{MSY} is better determined; however, the lower 1 SD bound also approaches zero. The predicted catch is reasonably determined in the data, and it is this parameter that is used in maximizing the likelihood function. The likelihood profiles (probability distributions) for the estimated parameters quantify the model's confidence in the values (see explanation of Bayesian inference in Section 3.3). Figures 45-47 show that the boundary constraints placed on these parameters in the model are constraining the likelihood profiles as well. Because the curves do not decrease substantially until they approach these bounds, we can conclude that these parameters are not well determined in the data. Note that *MSY* is a direct function of *k*, hence it has a proportional likelihood profile.

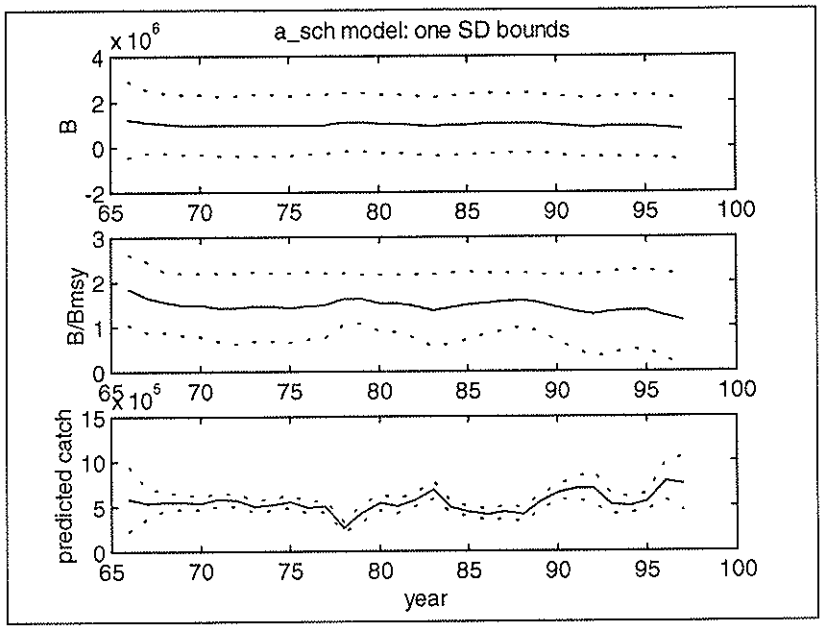

Figure 44. Scalar-*k* Model Output Time Series with 1-SD Bounds. 1SD bounds are moderate for predicted catch (moderate confidence) and wide for B and B/B_{MSY} (low confidence).

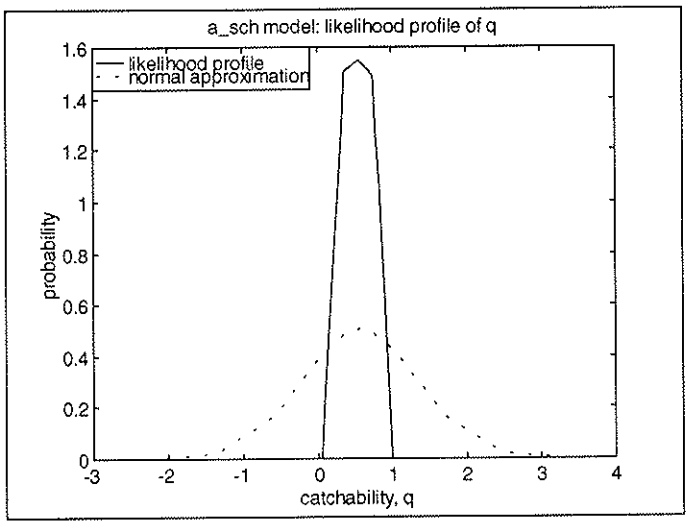

Figure 45. Likelihood Profile of 'q' for Akule

significance level	lower bound	upper bound
0.9	0.18366	0.894392
0.95	0.138797	0.929595
0.975	0.0957949	0.945822

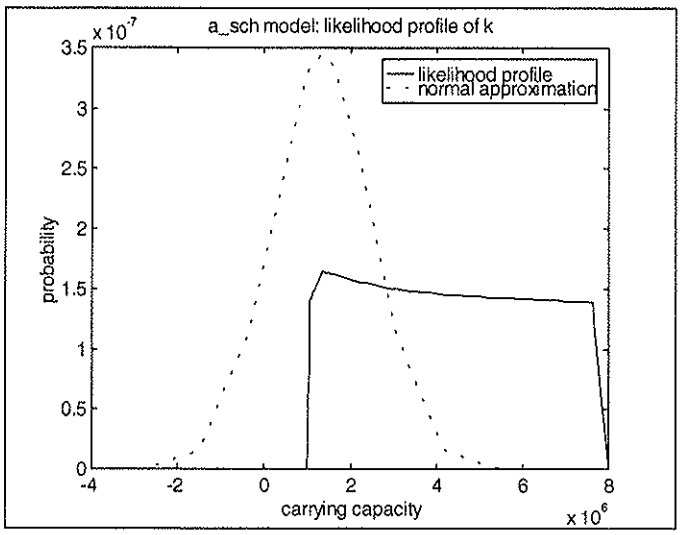

Figure 46. Likelihood Profile of 'k' for Akule

significance level	lower bound	upper bound
0.9	1.05726e+06	7.31065e+06
0.95	1.04908e+06	7.65821e+06
0.975	1.04179e+06	7.67976e+06

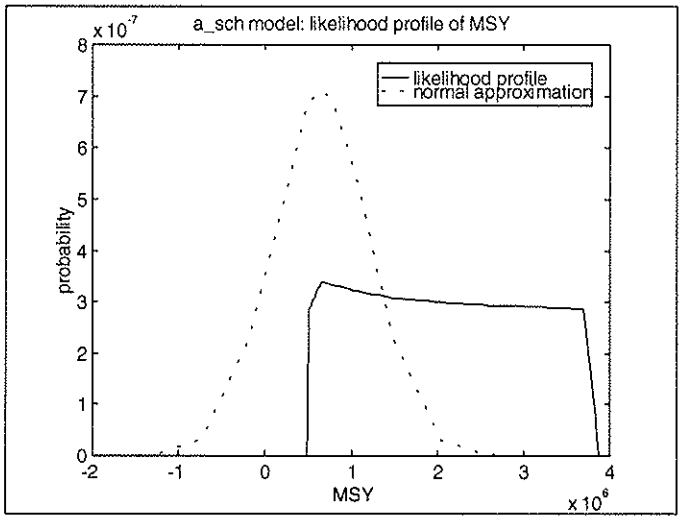

Figure 47. Likelihood Profile of *MSY* for Akule

significance level	lower bound	upper bound
0.9	512770	3.54566e+06
0.95	508802	3.71423e+06
0.975	505269	3.72468e+06

6.6.4 Vector-k Model for Akule

6.6.4.1 Output Parameters

Objective function value, log L = 1.59909
Catchability, q = 0.107577

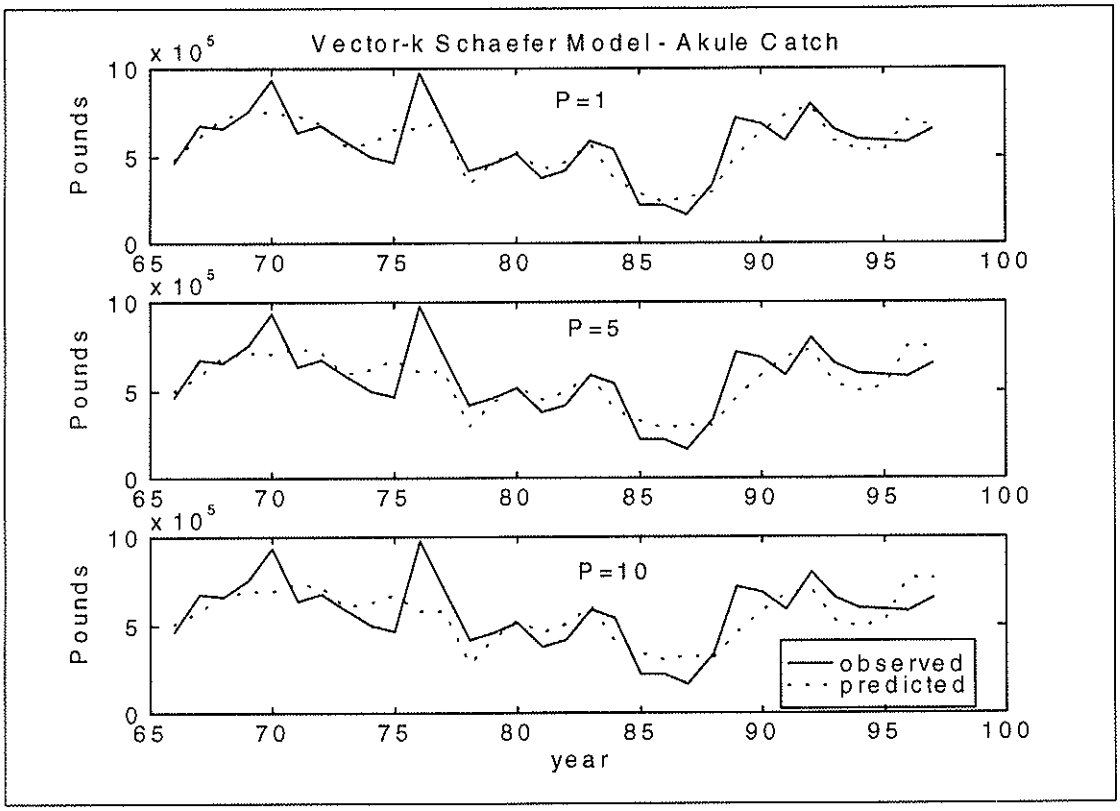

Figure 48. Observed and Predicted Catch for Akule Vector-*k* Model. Predicted catch is shown at three penalty levels, allowing different amounts of variation in carrying capacity (see text for explanation).

Figure 48 shows that the fit between observed and predicted catch becomes closer as the penalty is relaxed. The model's ability to vary k is diminished by the penalty. Lower penalization of variation in carrying capacity leads to higher variation in carrying capacity; note that magnitude is also higher. A scalar-k model must find the best compromise value of k for all times. The vector-k model can optimize k at each time, allowing higher overall k; as the penalty is relaxed, k becomes more optimized.

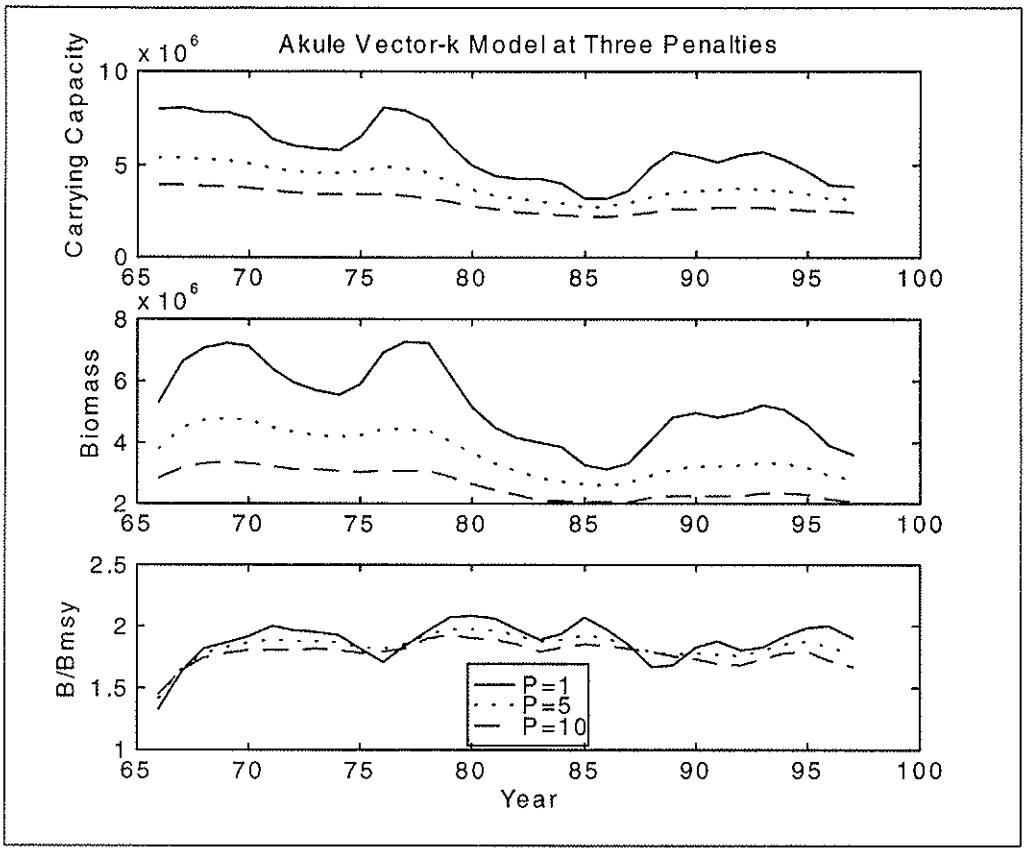

Figure 49. k, B and B/B_{MSY} for Akule Vector-k Model (note truncated y-axes). Time series are shown for three penalty levels, which allow different amounts of variation in carrying capacity (see text for explanation)

Figure 49 shows that the penalty affects biomass as it affects k: the time series for lower penalties are higher in both variance and magnitude. The models predict ratio time series that differ primarily in variation rather than trend or magnitude because a lower penalty leads to an increase in both B and B_{MSY}. A ratio in excess of one indicates a fishery exploited below *MSY*, which is a healthy fishery.

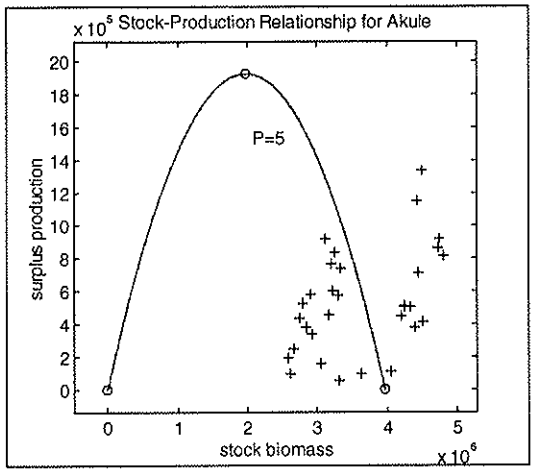

Figure 50. Surplus Production for Akule Vector-*k* Model. The point cloud covers a small portion of possible values, indicating the low contrast in the data.

The stock-production relationship of the Schaefer Model is plotted in Figure 50, as described for the akule scalar-*k* model above. Data are from the results under a penalty of five. Note that, as discussed in Section 6.2, the theoretical curve is based on the mean *k*-value. The output values are based upon *k* for each time, so the output values have high variance. While the points are dispersed, they are in the lower right region of the curve, indicating light exploitation. Negative values of surplus production result any time the biomass decreases and occur in the absence of fishing. Therefore, negative values are not necessarily indicative of overfishing.

6.6.4.2 Confidence in Results

Figures 51 and 52 show that B and k are poorly determined, as the 1 SD bounds include zero values. However, the B/B_{MSY} time series maintains itself between 1.5 and 2 and its 1SD bound does not pass below 1, indicating confidence that the stock is above B_{MSY}. The predicted catch is reasonably determined. Note that the model uses predicted catch to find the peak of the likelihood function.

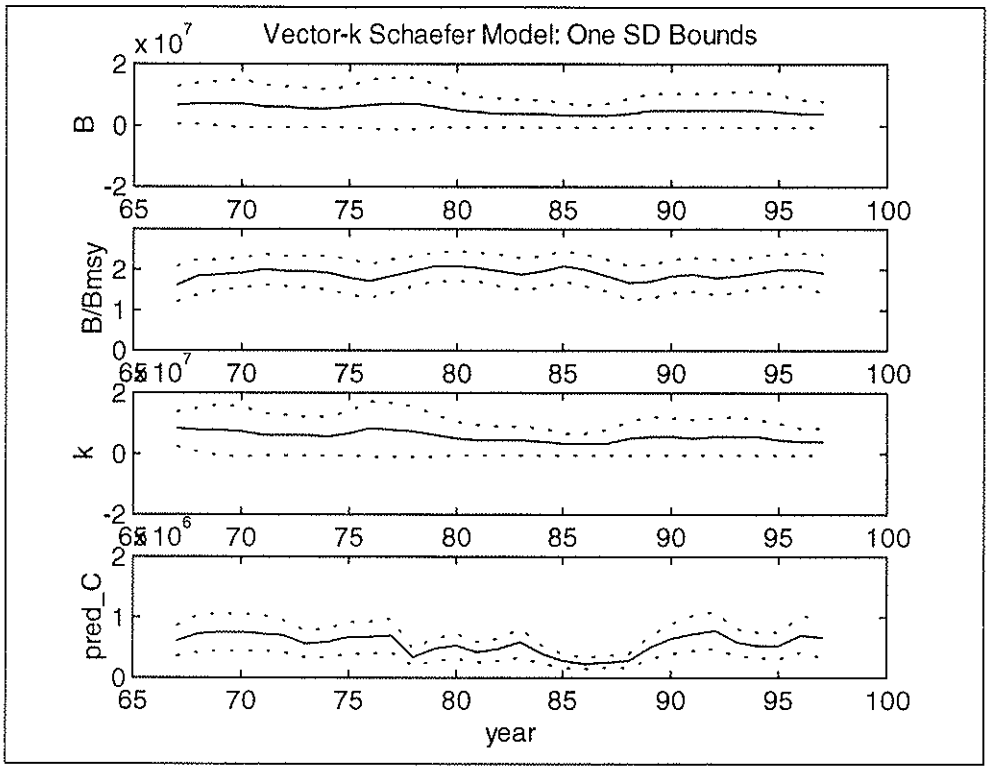

Figure 51. Vector-*k* Model—Output Time Series with 1-SD Bounds. Moderate bounds indicate moderate confidence in results.

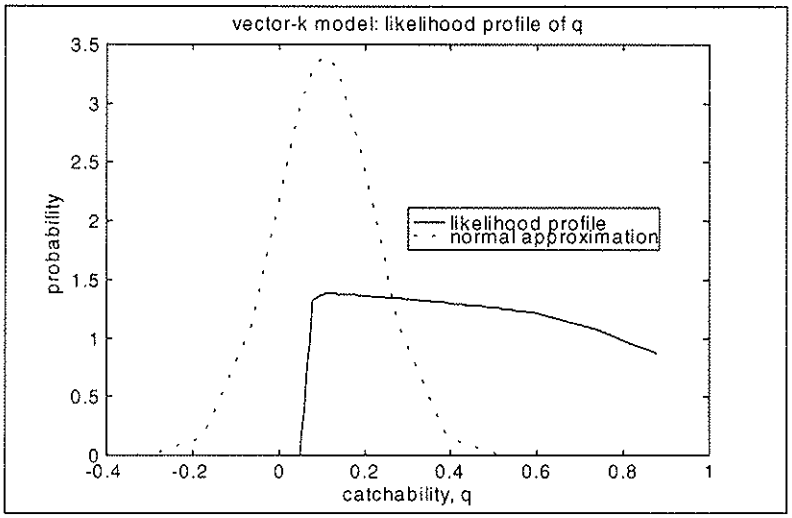

Figure 52. Vector-*k* Model—Likelihood Profile of 'q' for Akule

significance level	lower bound	upper bound
0.9	0.0707325	0.80383
0.95	0.066586	0.851739
0.975	0.065683	0.878473

The likelihood profiles for the estimated parameters quantify the model's confidence in the values (see explanation of Bayesian inference in Section 3.3) and shows that q is not well

determined in the data. To confirm the validity of the sum-of-squares method of calculating the likelihood function, the distribution of the estimates around the data were calculated and found to be normal.

6.6.5 Scalar-k Model for Opelu

6.6.5.1 Output Parameters

Figure 53 shows that the biomass has always been above B_{MSY}. Also note that the predicted catch is closely matched to the observed catch, indicating the model achieved a good fit.

Objective function value, log L = 1.218
Catchability, q = 0.370
Carrying capacity, k = 846372
Maximum sustainable yield, MSY = 393563

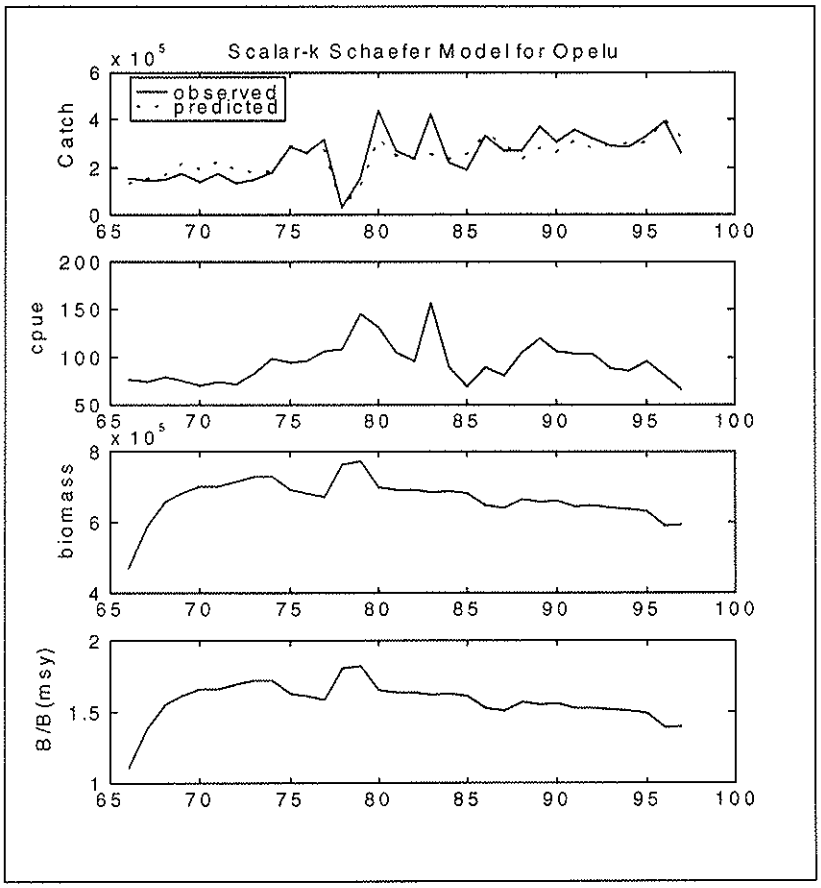

Figure 53. Scalar-*k* Model—Input and Output Time Series for Opelu. (Note truncated y-axes)

In Figure 54 the stock-production relationship shows that the point cluster is about midway between an unexploited fishery and one at *MSY*.

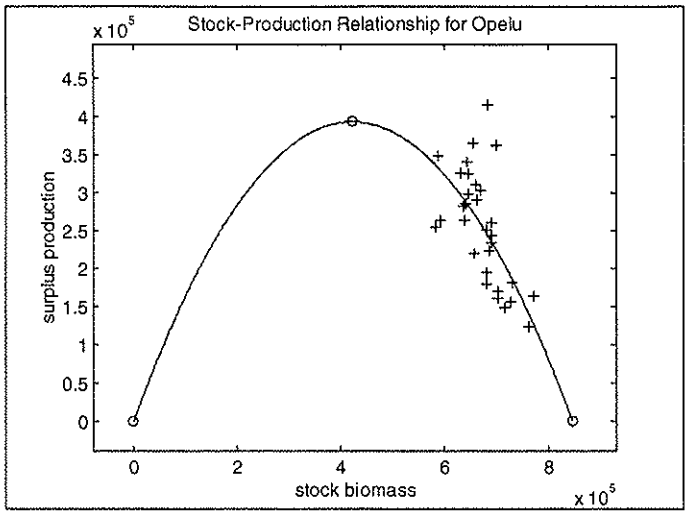

Figure 54. Scalar-*k* Model—Stock-Production Curve for Opelu. The point cloud covers a small range of values, due to the low contrast in the data.

6.6.5.2 Confidence in Results

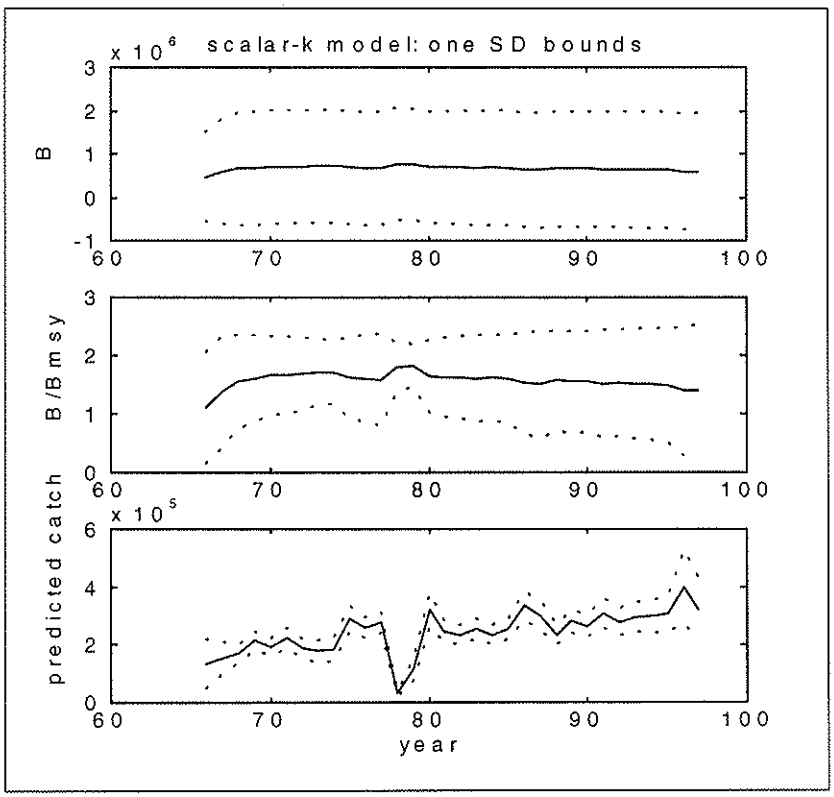

Figure 55. Scalar-*k* Model—Output Time Series for Opelu with 1-SD Bounds. 1SD bounds are moderate on predicted catch (moderate confidence) and wide on $\underline{B}$ and B/B_{MSY} (low confidence).

Figure 55 shows that the model does not determine B well. However, B/B_{MSY} and predicted catch are reasonably determined. The predicted catch is used in maximizing the likelihood function.

The likelihood profiles (Figures 56-58) for the estimated parameters quantify the model's confidence in the values (see explanation of Bayesian inference in Section 3.3). The likelihood profile for q reflects the restraints placed on its bounds in the model. *MSY* is a function of k.

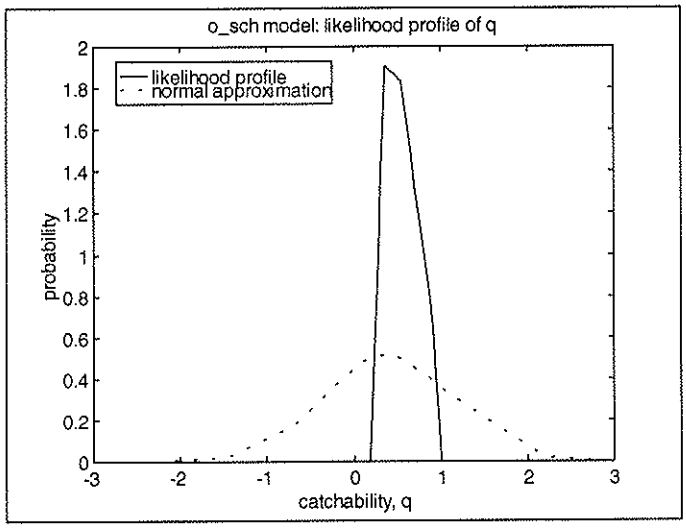

Figure 56. Scalar-*k* Model—Likelihood Profile of Catchability Parameter 'q' for Opelu

significance	lower bound	upper bound
0.9	0.109529	0.867396
0.95	0.0896858	0.928783
0.975	0.0871135	0.937848

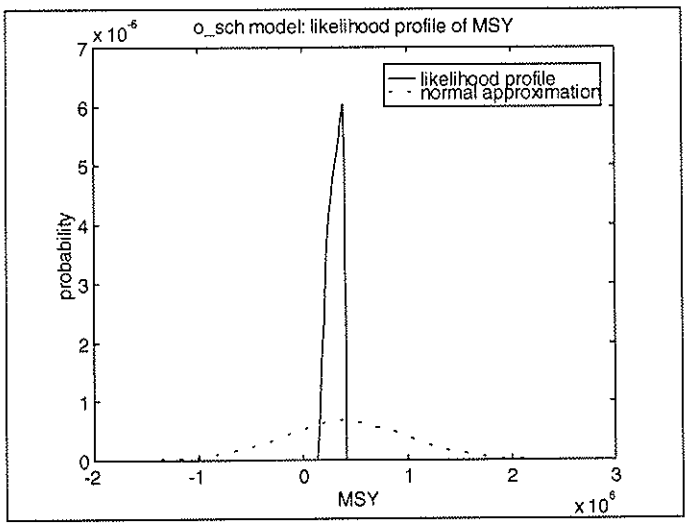

Figure 57. Scalar-*k* Model—Likelihood Profile of Maximum Sustainable Yield for Opelu

significance	lower bound	upper bound
0.9	170909	1.88838e+06
0.95	155204	2.23645e+06
0.975	139500	2.52163e+06

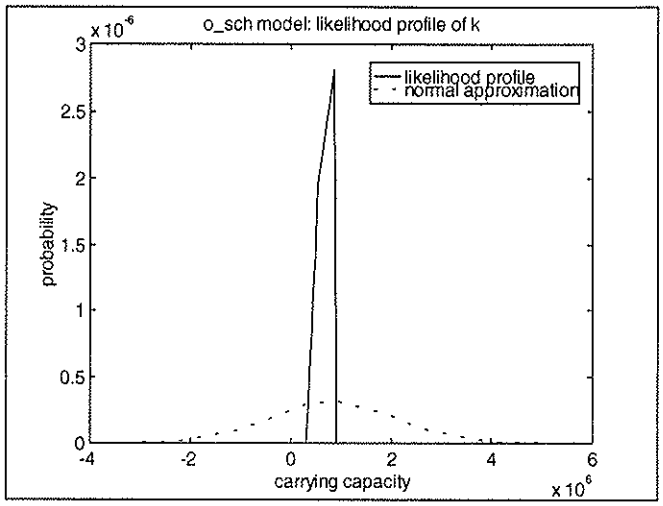

Figure 58. Scalar-*k* Model—Likelihood Profile of 'k' for Opelu

significance level	lower bound	upper bound
0.9	367545	4.06104e+06
0.95	333773	4.80957e+06
0.975	300000	5.42286e+06

Note that *k* is bounded in the model, forcing the likelihood profile to be narrow. If *k* is released from these bounds, it is evident that it is not well determined, as shown in Figure 59. Note that the confidence limits are the same, whereas the graph changes based on the bounds given in the model.

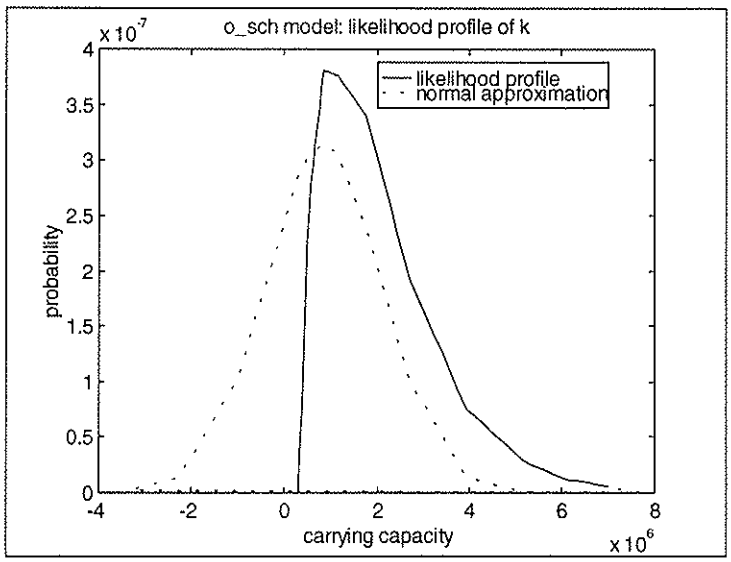

Figure 59. Scalar-*k* Model—Likelihood Profile of 'k' Without Boundary Constraints

significance level	lower bound	upper bound
0.9	367545	4.06104e+06
0.95	333773	4.80957e+06
0.975	300000	5.42286e+06

To confirm the validity of the sum-of-squares likelihood function used in this model, the distribution of the estimates around the data were calculated and found to be normal.

6.6.6 Vector-k Model for Opelu

6.6.6.1 Output Parameters

Objective function value, $\log L = 0.487$
Catchability, $q = 0.246$

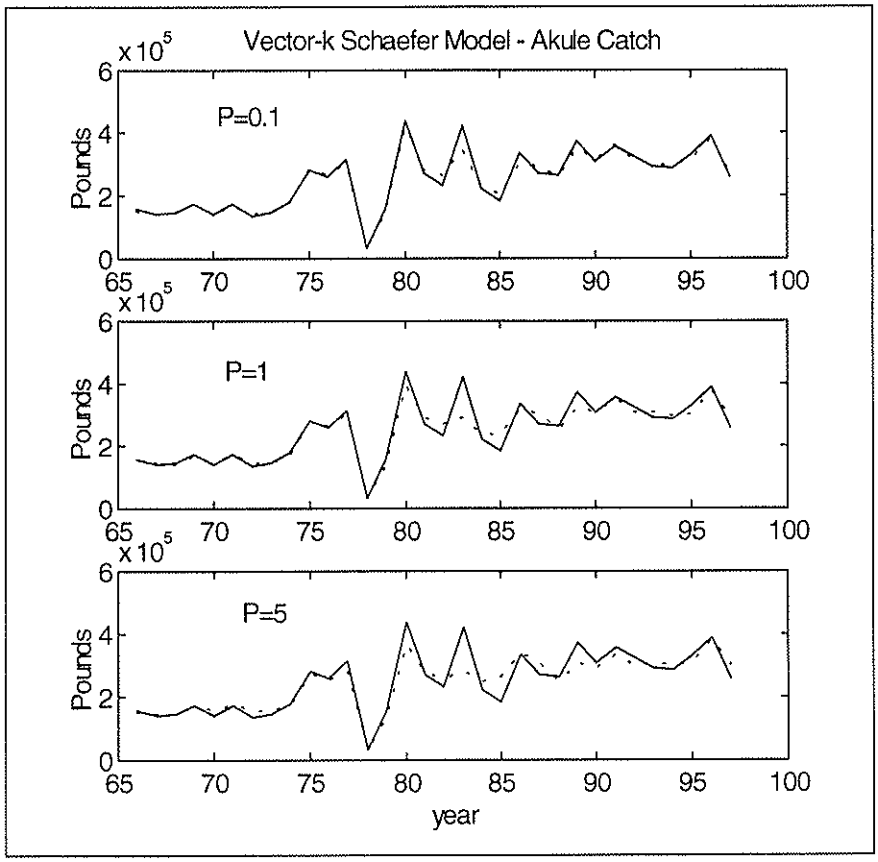

Figure 60. Vector-*k* Model—Observed and Predicted Catch for Opelu. Predicted catch is shown for three penalty levels, which allow different amounts of variation in carrying capacity.

Note the close fit between predicted and observed catch in Figure 60. The model achieves a closer fit for the opelu than for the akule.

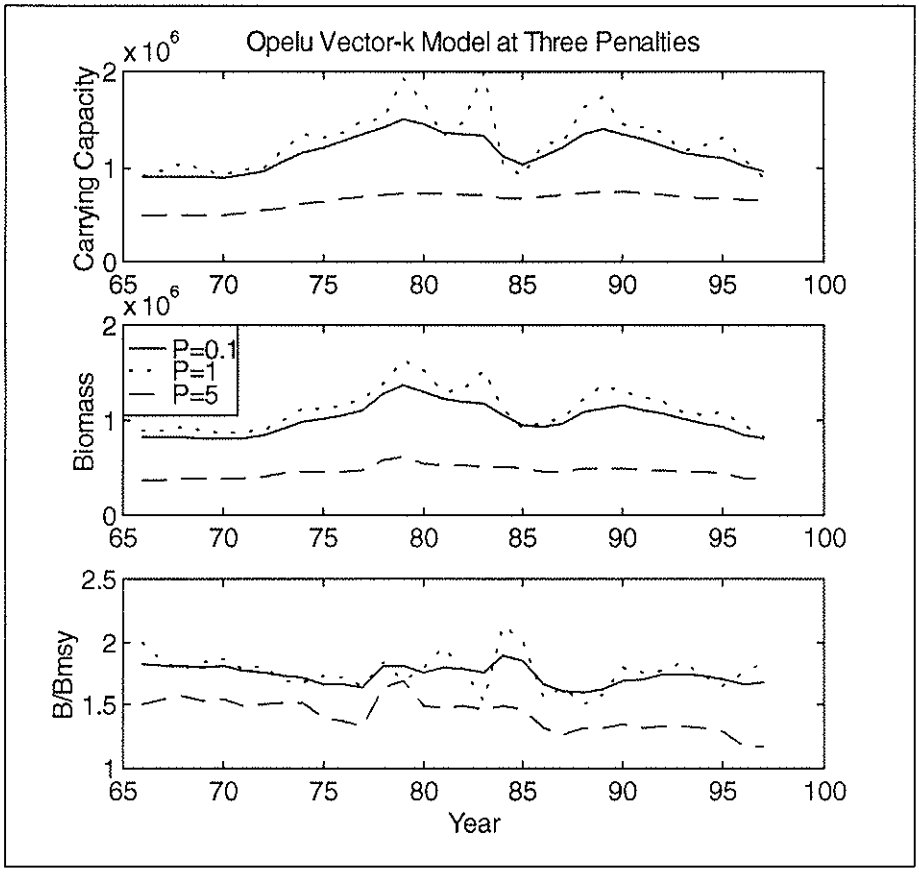

Figure 61. Vector-*k* Model—*k*, *B* and B/B_{MSY} for Opelu. Time series are shown for three penalty levels, which allow different amounts of variation in carrying capacity (note truncated y-axes).

The pattern in Figure 61 differs from that of the akule in that the B/B_{MSY} ratio is lower for the higher penalty value.

The stock-production relationship of the Schaefer Model is plotted in Figure 62, in the same manner as described for the akule scalar-*k* model. Data are from the results under a penalty of five. The range of the point cluster is slightly to the left of *k*, indicating light exploitation.

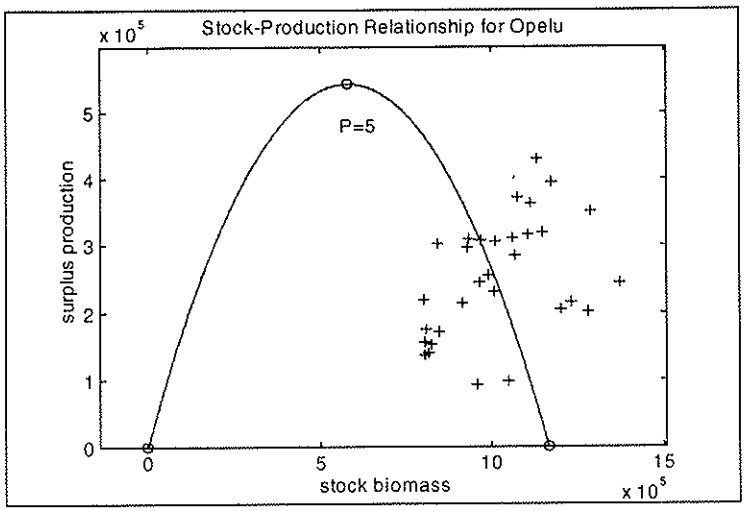

Figure 62. Vector-*k* Model—Stock-Production Relationship for Opelu. The point cloud covers a small portion of possible values, indicating the low contrast in the data.

6.6.6.2 Confidence in Results

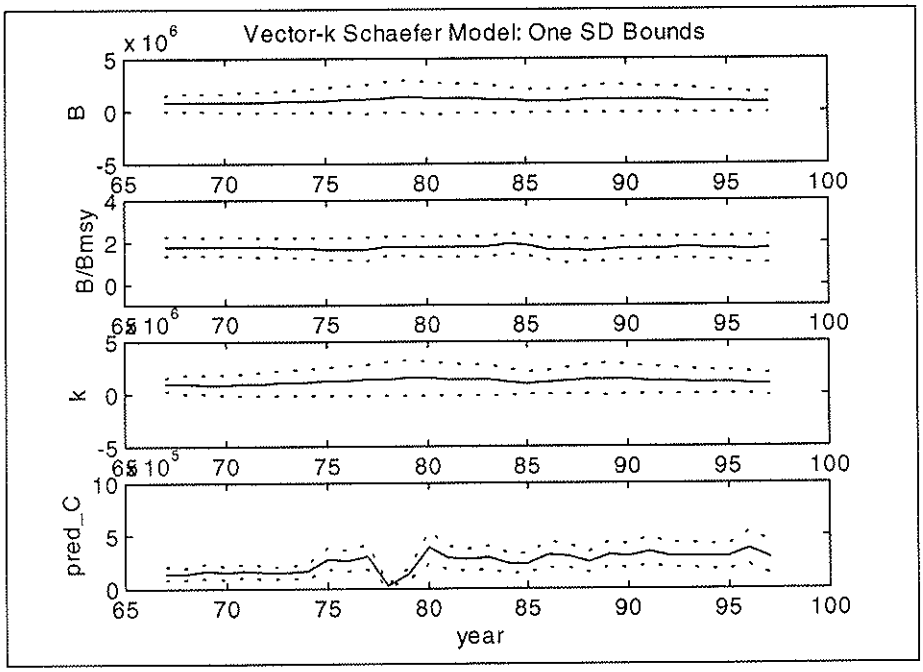

Figure 63. Vector-*k* Model—Output Time Series with 1-SD Bounds for Opelu. Moderate bounds indicate moderate confidence in results.

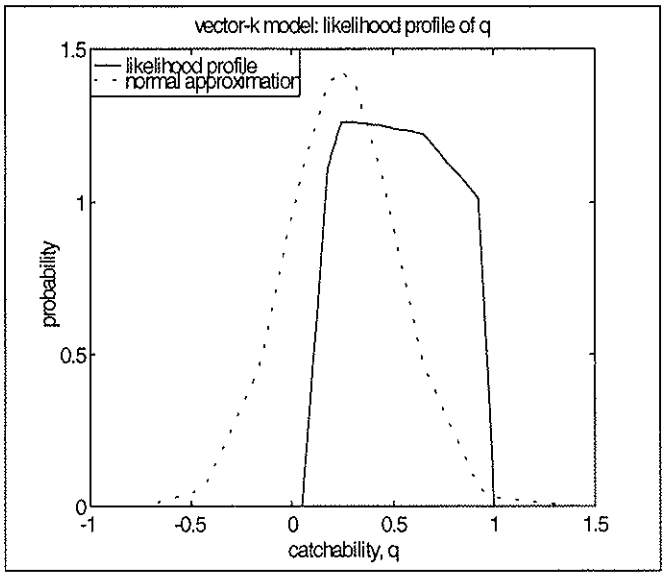

Figure 64. Vector-*k* Model—Likelihood Profile of 'q' for Opelu

significance level	lower bound	upper bound
0.9	0.160057	0.957131
0.95	0.123371	0.949496
0.975	0.101152	0.967578

Figures 63 and 64 show that B and k are poorly determined in the vector-k model, while B/B_{MSY} and predicted catch are better determined. The one standard deviation bound of B/B_{MSY} is above one for the entire time series, with the ratio itself lying at approximately 1.7. Predicted catch undergoes considerable variability, with the one standard deviation bound lying above zero for the entire time series. Note that the predicted catch is used in maximizing the likelihood function. The likelihood profiles for the estimated parameters quantify the model's confidence in the values (see explanation of Bayesian inference in Section 3.3).

To confirm the validity of the sum-of-squares likelihood function used in this model, the distribution of the estimates around the data were calculated and found to be normal.

6.7 Carrying Capacity and Environmental Variability

6.7.1 Background

The vector-k model determines the most likely time series of k based on the input fishery time series, without reference to external factors. In order for the resulting changes in k to have significance, the existence of a plausible causal mechanism must be demonstrated. Therefore, the time series of k generated for akule and opelu are correlated with two classes of variables that have potential interactions with them. Variables of the physical environment comprise the first class. The physical environment may affect the productivity of the marine environment where the small pelagic fishes live, the ecological processes therein, or the recruitment and growth success of these fishes. Ecological variables comprise the second class and consist of abundance data for large pelagic fishes captured in the nearshore environment. Large pelagic fishes prey on akule and opelu and there is the possibility that the population dynamics of the predator may affect the prey, or vice versa.

The time series for akule, opelu, and environmental variables are differenced with a lag of one. Differencing replaces each value by the difference between it and the next value. The effect is to remove trend from the time series, which can lead to false positives. These detrended time series are then correlated with the Pearson correlation (r) using a range of lag times. A correlation of $| r | > 0.5$ is considered the minimum required for consideration of possible causal linkages because the majority of variability in the fishery time series is explained by variability in the environmental time series. The two time series being correlated may be lagged relative to one another. If the akule is lagged by one year, the time series is shifted one year into the future. The 1997 value is compared to the 1996 value for the environmental variable, and so on. Correlations with lags greater than three years are not considered because neither the akule nor opelu survives to greater than three years of age for a significant portion of the population (Froese and Pauly 1998) and, therefore, environmental influence cannot exceed this time.

6.7.2 Physical Variables

The time series of k for akule and opelu are cross-correlated with time series for the following physical variables:

- sea surface temperature and anomaly
- wind strength and anomaly
- sea level anomaly
- ocean current strength
- air temperature (terrestrial)
- total precipitation (terrestrial).

The akule carrying capacity time series is correlated with total precipitation (r=0.59). Precipitation is lagged two years behind akule k. The k-time series is generated at a penalty level of 0.1. For the undifferenced time series, r=0.69.

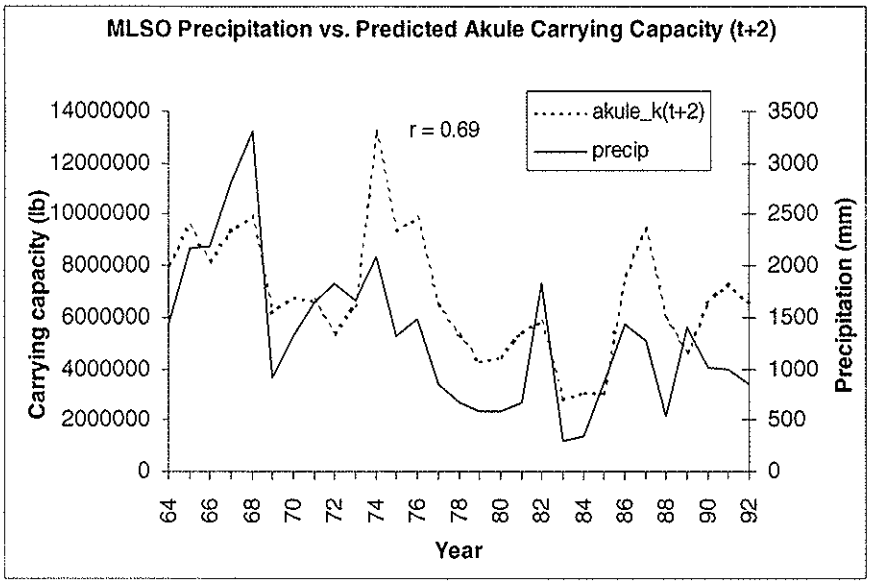

Figure 65. Correlation of Mauna Loa Precipitation and Akule *CPUE*. The akule carrying capacity time series is lagged two years after precipitation, which is approximately the time required to reach maximum length. Hence, this relationship may indicate that climatic effects on larvae are reflected in adult population two years later.

In Figure 65 it is evident that the time series for k and precipitation show similarity in both the trend and magnitude of change.

6.7.3 Ecological Variables

The time series of k for akule and opelu are cross-correlated with time series for the following ika shibi species.

- bigeye
- bluefin
- yellowfin
- albacore
- swordfish
- black marlin
- blue marlin
- kawakawa
- mahimahi
- ono
- sailfish
- skipjack
- spearfish
- striped marlin

The akule and opelu did not show strong correlation with any of the ika shibi species.

6.8 Discussion

6.8.1 Test Cases: Confirmation of Model's Diagnostic Ability

The test cases for the scalar and vector-k models show that both versions correctly diagnose a crashing fishery with minor errors. Error in the scalar-k model causes premature prediction of *MSY* and, therefore, adds a precautionary margin. The vector-k model lags in predicting *MSY*, but this lag is a foregone conclusion because the input data for this scenario assumes constant k. This result is important because it highlights the risks inherent in using this approach without

independent evidence of variation in k-changes in *CPUE* that are due to other factors are masked by changes in k.

6.8.2 Sources of Uncertainty

The good performance of both versions of the model under an idealized scenario shows that it can diagnose the condition of a fishery with good precision and moderate accuracy. However, there are a number of sources of uncertainty that reduce performance under real-world conditions.

First and foremost is the lack of contrast in most fishery data sets, the akule and opelu included. Many fisheries data sets miss the developmental stage in a fishery where $B \sim k$, so the data lacks points on the far right of the stock-production curve. Alternately, if B is much lower than B_{MSY}, we have points on the far left of the stock-production curve. However, it may already be too late for sustainable management because recruitment overfishing has likely been occurring for some time. Inclusion of these two conditions is necessary in order to have a high contrast data set. Their absence is one of the primary causes of uncertainty in fishery assessments. Hilborn and Walters (1992) stress the seemingly obvious, but sometimes neglected, fact that we cannot tell how a stock will respond to heavy fishing until it has been heavily fished.

A low contrast data set can be consistent with virtually any condition: low exploitation, high biomass, low surplus production; optimal exploitation, moderate biomass, maximum surplus production; and overexploitation, low biomass, and low surplus production. If the database lacks more than one condition, we cannot confidently situate the fishery along this continuum. The method does allow assessments of stock status to be made, because we can produce stock-production relationships and B/B_{MSY} time series. However, the lower the contrast, the less confident these estimates.

The catchability parameter, q, is another source of uncertainty. In the Schaefer Model, predicted catch given by $\hat{C} = qEB$. Because both q and B are unknown, there are too many degrees of freedom for an analytical solution. Therefore, the numerical solutions used here are required. However, confident solutions are again dependent upon the data. The likelihood profiles show that q is poorly determined in both akule and opelu data when compared to the test cases.

The population growth parameter, r, is constant in the models used here. However, the values used are a source of uncertainty. Values for r are calculated from K and W_∞, with W_∞ itself being a function of L_∞. In addition, the empirical constants used in the equation for r also contain error.

6.8.3 Akule

The scalar-k model indicates that the akule fishery has moderately low contrast. The surplus production plot (Figure 43) shows that the data missed the development of the fishery when B was at or near k, as represented by the lower right end of the theoretical curve. Most of the points lie about 2/3 of the way from k to B_{MSY}, indicating exploitation below *MSY*. Heavy exploitation is not represented, as there are no points at B-values
lower than B_{MSY}. The B/B_{MSY} plot in Figure 42 shows an overall decline from about 1.5 to 1.2, indicating that the catch is increasing towards *MSY*.

The vector-k model also indicates low contrast because the points reside in the lower right portion of the stock-production plot (Figure 50). Note that the spread of the points increases due to the variation in k, while the theoretical curve is based on mean-k. Lower penalty values allow higher variation in and magnitude of k and, therefore, B and MSY. However, the overall conclusion from this model is best seen in the B/B_{MSY} plot, which does not undergo much long term change, and remains at a mean of about 1.8 through the time series. The decline in *CPUE* has been explained by a decline in k. Before such a result can be used with confidence, independent estimates of variation in k are needed.

6.8.4 Opelu

The scalar-k model achieves a closer fit for opelu than for akule (note the lower objective function value and the closer fit of predicted catch to observed catch). The surplus production plot (Figure 54) indicates low contrast, again missing the developmental stage of the fishery, and shows no evidence of heavy fishing pressure at or above MSY. The B/B_{MSY} plot in Figure 53 makes an early increase to about 1.7 then falls very gradually to about 1.4.

The vector-k model also indicates light exploitation, with the points about 1/3 of the way from k to B_{MSY}. Note that unlike the akule vector-k results, changes in penalty weight change the magnitude and trend of the B/B_{MSY} time series. With low variation in k, B/B_{MSY} declines from about 1.6 to 1.2, indicating that catch is approaching MSY. In the higher variation k scenarios the ratio is higher and the decline very minor, moving from about 1.9 to 1.75. This is because the opelu *CPUE* does not have a monotonic trend, so the vector-k model is unable to incorporate its variability at high penalties.

6.8.5 Correlations with Environmental Variables

The precipitation at Mauna Loa is correlated with the k time series for akule lagged by two years. The k time series was generated using a penalty weight of 0.1, which allows a high degree of variability in k. Given the one-year generation time and high growth rate of the akule, it is anticipated that environmental changes could be translated into changes in biomass on a one to two-year time scale, so high variability in k is an appropriate assumption. Given the two to three year life span of the akule, the two-year lag time would be expected if variation in precipitation affected recruitment success or early development. Precipitation is strongly correlated with terrestrial runoff to the coastal ocean, which is in turn a source of fertilization to the otherwise oligotrophic waters of the North Pacific subtropical gyre. In addition, precipitation scrubs various chemicals out of the atmosphere and deposits them in the ocean. Hence, there is a plausible mechanism of interaction between precipitation and akule population dynamics.

6.9 Conclusions

The best available model fitting techniques and powerful statistical methods are used to analyze the akule and opelu data. The test cases show that the models are able to correctly diagnose a declining fishery, given a high contrast data set. The use of these
models in real-world situations incurs a range of sources of uncertainty associated with low contrast data, the catchability parameter, and the population growth parameter.

Results for the scalar-k model suggest that the akule population has undergone moderate exploitation, and that the biomass is approaching B_{MSY}, but remains about 20% above it. The vector-k model indicates that the akule has undergone light exploitation, and that the biomass has

remained about 80% greater than B_{MSY} through the time series. The decrease in *CPUE* is due to a decrease in biomass. Results for the scalar-*k* model indicate that the opelu has undergone light to moderate exploitation, and that the biomass has declined gradually but remains about 40% greater than B_{MSY}. The confidence is higher than for the akule data. Results for the vector-*k* model show a range of scenarios from one similar to the scalar-*k* results to one in which biomass has declined less during the time series, remaining at about 75% greater than B_{MSY}.

The one standard deviation bounds on B/B_{MSY} pass below a value of one in the scalar-*k* model for both akule and opelu, raising the possibility that the stocks may be overfished within this range of certainty. These bounds remain above one for both species in the vector-*k* model. While this is a high level of uncertainty, the use of such models on a low contrast database does not allow for any other outcome. A lightly exploited fishery will always have a low contrast data set. Therefore, the results are consistent with a light to moderate exploitation at levels below *MSY*.

Using a vector-*k* model involves greater risks than using a scalar-*k* model, because the former is able to account for decreases in *CPUE* by reducing *k*, regardless of whether *k* actually falls. Thus, the results of vector-*k* models should be treated with caution unless independent evidence exists that changes in *k* are real. Correlations with numerous physical and fishery variables highlighted total precipitation at Mauna Loa. Precipitation may influence carrying capacity through the fertilization of the coastal ocean via terrestrial runoff and atmospheric scrubbing. This presents a hypothesis to be tested in future research.

REFERENCES

Alcala, A., and G. Russ. 1990. A direct test of the effects of protective management on abundance and yield of tropical marine resources. *J. Cons., Cons. Int. Explor. Mer* 46: 40-47.

Boehlert, G., and B. Mundy. 1996. Ichthyoplankton vertical distributions near Oahu, Hawaii, 1985-1986: Data Report. NMFS NOAA-TM-NMFS-SWFSC-235. *NOAA Technical Memorandum.*

Bohnsack, J. 1996. Maintenance and recovery of reef fishery productivity. *In* N. Polunin and C. Roberts, eds. *Reef Fisheries*. Chapman & Hall, London, p. 283-313.

Brownlee, K. 1965. *Statistical Theory and Methodology in Science and Engineering*. John Wiley & Sons, New York.

Cervigón, F. 1993. *Los peces marinos de Venezuela*. Fundación Científica Los Roques, Caracas, Venezuela.

Chirichigno, N. 1974. Clave para identificar los peces marinos del Peru. *Inf. Inst. Mar Perú* 44: 387.

Clarke, T., and L. Privitera. 1995. Reproductive biology of two Hawaiian pelagic carangid fishes, the big-eye scad, *Selar crumenopthalmus*, and the round scad, *Decapterus macarellus*. *Bull. Mar. Sci.* 56: 33-47.

Dalzell, P., and G. Penaflor. 1989. The fisheries biology of the big-eye scad, *Selar crumenopthalmus* (Bloch) in the Philippines. *Asian Fisheries Science* 3: 115-131.

DeMartini, E. 1993. Modeling the pontential of fishery reserves for managing pacific coral reef fishes. *Fish. Bull.* 91: 414-427.

Department of Land and Natural Resources, State of Hawaii, 1999. Internet resource *http://www.hawaii.gov/dlnr/dar/bottomfish.html.*

Fournier, D. 1996. AD Model Builder. Otter Research Ltd., Nanaimo, BC.

Fournier, D. 1999. Internet resource *http://www.island.net/~otter/admodel.htm*

Froese, R., and D. Pauly, eds. 1998. *FishBase 98 (CD-ROM)*. International Centre for Living Aquatic Resources Management, Manila.

Gordon, D., and G. Munro, eds. 1994. *Fisheries and uncertainty: a precautionary approach to resource management*. University of Calgary Press, Calgary.

Gushiken, S. 1983. Revision of the Carangid fishes of Japan. *Galaxea* 2: 135-264.

Hilborn, R., and C.J. Walters. 1992. *Quantitative Fisheries Stock Assessment. Choice, Dynamics, Uncertainty.* Chapman and Hall, New York.

Hughes, T. 1994. Catastrophes, phase shifts, and large-scale degredation of a Caribbean coral reef. *Science* 265: 1547-1551.

Iri, M. 1991. History of automatic differentiation and rounding error estimation. *In* A. Griewank and G. Corliss, eds. *Automatic Differentiation of Algorithms: Theory, Implementation and Application*. Society for Industrial and Applied Mathematics, Philadelphia, p. 3-16.

Iwai, T. J., C. Tamaru, L. Yasukochi, S. Alexander, R. Yoshimura, and M. M. 1996. Natural spawning of captive bigeye scad *Selar crumenopthalmus* in Hawaii. *J. World Aquaculture Soc.* 27.

Kawamoto, P. 1973. Management investigation of the akule or big-eye scad, *Trachurops crumenopthalmus* (Bloch). Hawaii Div. Fish. Game.

O'Hagan, A. 1994. *Bayesian Inference*. Edward Arnold, Hodder Headline PLC, London.

Petersen, C. 1895. Eine Methode zur Bestimmung des Altres and Wuchsesder Fische. *Mittheilunges, Deutchen Seefishereivereins (Fide Van Oosten, 1929)* 11: 226-235.

Podosinnikov, A. 1990. Information on the development of scads in the Gulf of Aden. *J. Ichthyol.* 30: 158-164.

Polacheck, T. 1990. Year around closed areas as a management tool. *Natural Resource Modeling* 4: 327-353.

Powell, R. 1968. Hawaiian Opelu hoop net fishing gear. South Pacific Commission, Noumea, New Caledonia.

Robert, C. P. 1994. *The Bayesian Choice: A Decision-Theoretic Motivation*. Springer-Verlag, New York.

Roberts, C. 1997. Connectivity and management of Carribean coral reefs. *Science* 278: 1454-1457.

Schaefer, M. 1954. Some aspects of the dynamics of populations important to the management of commercial marine fisheries. *Bulletin Inter-American Tropical Tuna Commission* 1: 27-56.

Schmitt, S. A. 1969. *Measuring Uncertainty: An Elementary Introduction to Bayesian Statistics*. Addision-Wesley, Reading, MA.

Schultz, L., E. Herald, E. Lachner, A. Welander, and L. Woods. 1953. Fishes of the Marshall and Marianas Islands. US National Museum.

Smith-Vaniz, W. 1984. Carangidae. *In* W. Fischer and G. Bianchi, eds. *FAO Species Identification Sheets for Fishery Purposes. Western Indian Ocean Fishing Area 51. Vol. 1.* FAO, Rome.

Smith-Vaniz, W. 1986. Carangidae. *In* P. Whitehead, M. Bauchot, J. Hureau, J. Nielsen, and E. Tortonese, eds. *Fishes of the North-Eastern Atlantic and the Mediterranean*. UNESCO, Paris.

Smith-Vaniz, W. 1995. Carangidae. *In* W. Fischer, F. Krupp, W. Schneider, C. Sommer, K. Carpenter, and V. Niem, eds. *Guia FAO para Identification de Especies para lo Fines de la Pesca. Pacifico Centro-Oriental. 3 vols.* FAO, Rome.

Smith-Vaniz, W., J. Quéro, and M. Desoutter. 1990. Carangidae. *In* J. Quero, J. Hureau, C. Karrer, A. Post, and L. Saldanha, eds. *Check-List of the Fishes of the Eastern Tropical Atlantic (CLOFETA).* JNICT, Lisbon; SEI, Paris; and UNESCO, Paris.

Sullivan, K. 1991. The estimation of parameters of the multispecies production model. *ICES Mar. Sci. Symp.* 193: 185-193.

Tobias, W. 1987. Resource evaluation of the bigeye scad, *Selar crumenopthalmus* (Bloch), in the insular shelf waters around St. Croix, U.S. Virgin Islands. *Proceedings of the Fortieth Annual Gulf and Caribbean Fisheries Institute, Curacao Netherlands Antilles, November 1987., 1991., pp. 82-98, Proc. Gulf Caribb. Fish. Inst.*

Yamaguchi, Y. 1953. The fishery and the biology of the Hawaiian Opelu, *Decapterus Pinnulatus* (Eydoux ans Souleyet). University of Hawaii at Manoa, USA.